FLOW AND SOLUTE-TRANSPORT MODELS FOR THE NEW RIVER IN THE NEW RIVER GORGE NATIONAL RIVER, WEST VIRGINIA

By Jeffrey B. Wiley

U.S. GEOLOGICAL SURVEY

Open-File Report 92-65

Prepared in cooperation with the

NATIONAL PARK SERVICE

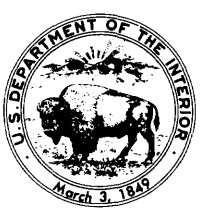

Charleston, West Virginia

1992

U.S. DEPARTMENT OF THE INTERIOR

MANUEL LUJAN, JR., Secretary

U.S. GEOLOGICAL SURVEY

Dallas L. Peck, Director

For Additional Information
write to:

District Chief
U.S. Geological Survey
603 Morris Street
Charleston, WV 25301

Copies of this report can be
purchased from:

U.S. Geological Survey
Books and Open-File Reports Section--ESIC
Denver Federal Center, Box 25425
Denver, CO 80225

CONTENTS

ILLUSTRATIONS

TABLES

TABLES--Continued

CONVERSION FACTORS, VERTICAL DATUM, AND UNITS OF CHEMICAL CONCENTRATION

Multiply	By	To obtain
inch (in.)	25.4	millimeter
foot (ft)	0.3048	meter
square foot (ft^2)	0.09294	square meter
mile (mi)	1.609	kilometer
square mile (mi^2)	2.590	square kilometer
gallon (gal)	3.785	liter
acre-foot (acre-ft)	1,233	cubic meter
foot per second (ft/s)	0.3048	meter per second
cubic foot per second (ft^3/s)	0.02832	cubic meter per second
pound (lb)	453.6	gram

Sea level: In this report, "sea level" refers to the National Geodetic Vertical Datum of 1929--a geodetic datum derived from a general adjustment of the first-order level nets of the United States and Canada, formerly called Sea Level Datum of 1929.

Chemical concentration: In this report, chemical concentration is given in micrograms per liter (µg/L). Micrograms per liter is a unit expressing the concentration of chemical constituents in solution as weight (micrograms) of solute per unit volume (liter) of water. One thousand micrograms per liter is equivalent to one milligram per liter.

FLOW AND SOLUTE-TRANSPORT MODELS FOR THE NEW RIVER IN THE NEW RIVER GORGE NATIONAL RIVER, WEST VIRGINIA

by Jeffrey B. Wiley

ABSTRACT

This report presents the results of a study by the U.S. Geological Survey (USGS), in cooperation with the National Park Service, to apply flow and solute-transport models to the New River in the New River Gorge National River, West Virginia. Relations between cross-sectional area and discharge developed from input parameters of an unsteady-flow model were compared to relations between cross-sectional area and discharge developed from a steady-flow model output. The study reach, 53 miles of the lower New River from Hinton to Fayette, is characterized as a pool-and-riffle stream that narrows, steepens, and deepens in the downstream direction. Three subreaches--Hinton to Meadow Creek, Meadow Creek to Sewell, and Sewell to Fayette--represented similar slopes, geometries, and roughness of the study reach.

A USGS steady-flow model, WSPRO (Water Surface PROfile), was applied to the study reach. The model was calibrated by use of relations developed between river stages and discharges. Cross-section configurations were determined by means of aerial photography, topographic maps, rating curves, and water-surface and streambed profiles. The model was verified by comparing random predicted water-surface elevations at a discharge of 2,000 ft^3/s (cubic feet per second) to those of a surveyed profile. The model was more sensitive to changes in Manning's roughness coefficients than to changes in the hydraulic-depth breakpoints corresponding to Manning's roughness.

A USGS unsteady-flow model, DAFLOW (Diffusion Analogy FLOW), and a USGS solute-transport model, BLTM (Branch Lagrangian Transport Model), were also applied to the study reach. Difficulty in calibration required development of separate models for discharges greater than or equal to 8,000 ft^3/s (high-discharge model) and less than or equal to 8,000 ft^3/s (low-discharge model). The DAFLOW models were calibrated by use of relations between river discharges and traveltimes of the change in discharge at the leading edge of waves. The DAFLOW models were verified by predicting discharges at the streamflow-gaging station at Thurmond using discharges from the Hinton station. The BLTM models were calibrated by use of relations between traveltime of peak concentration and discharge, and peak concentration and traveltime of peak concentration. The BLTM models were verified by predicting peak concentrations and traveltimes of peak concentrations for two unsteady-flow and one steady-flow dye measurements.

Relations between cross-sectional area and discharge, developed from calibration parameters for the steady-flow and unsteady-flow models, were compared. No explanation could be determined for the poor comparisons.

INTRODUCTION

The New River flows northward from its headwaters in North Carolina, through western Virginia, and into south-central West Virginia, where it joins the Gauley River to form the Kanawha River (fig. 1). The New River Gorge National River was established by Public Law 95-625 on November 10, 1978, and falls within jurisdiction of the U.S. Department of Interior, National Park Service (NPS) (fig. 2). The NPS is responsible for (1) conserving the natural, scenic, and historical objects, and (2) preserving a 53-mile segment of the lower New River (approximately from Hinton to Fayette) in West Virginia as a free-flowing stream for the enjoyment and benefit of present and future generations. The main attraction of the National River is a combination of scenic wilderness, fishing, and excellent white-water rafting. The recreational quality of the New River depends, in part, on the regulated flow from Bluestone Dam and unregulated flow from the Greenbrier River.

The U.S. Geological Survey (USGS), in a study made in cooperation with the NPS, applied flow and solute-transport models to the New River in the New River Gorge National River to investigate the capability of two separate models to represent an identical study reach by similar hydraulics.

The purpose of this report is to present comparisons of relations between cross-sectional area and discharge determined from calibration parameters used in the unsteady-flow model to relations of cross-sectional area and discharge determined from quantities calculated from the steady-flow model output. Calibration, verification, and sensitivity of applied models are discussed. The study area is limited to the main stem of the New River within the National River boundaries.

DESCRIPTION OF STUDY REACH

The study reach extends for 53 mi from Hinton to Fayette in the New River Gorge National River, West Virginia. The study reach narrows, steepens, and deepens in the downstream direction. Flow in the New River is partially regulated by Bluestone Dam.

The streamflow-gaging station at Hinton is the most upstream location in the study reach. The contributing drainage area is 6,256 mi^2 (Mathes and others, 1982), of which 4,601 mi^2 is regulated by Bluestone Dam (figs. 1 and 2). Approximately 1.5 mi upstream from the Hinton streamflow-gaging station and about 1.0 mi downstream from Bluestone Dam is the confluence with the Greenbrier River. The Greenbrier River is an unregulated stream with a drainage area of 1,641 mi^2. The most downstream point of the study reach is 53 mi from the Hinton streamflow-gaging station; the contributing drainage area at this point is approximately 6,872 mi^2. The additional drainage area within the study reach is about 600 mi^2. Approximately 360 mi^2 of this additional drainage area is accounted for by six small basins (five that range from 28 to 63 mi^2 and one that is 135 mi^2). The remaining inflows are primarily small tributaries that drain less than 5 mi^2.

Channel cross sections for discharges of 2,000 ft^3/s (a "low flow" discharge) can be described as trapezoids. The long base is three times the length of the short base, and the distance between the bases represents the stream depth. The 53-mile study reach can be divided into three subreaches of similar slope, geometry, and roughness (fig. 3): Hinton to Meadow Creek (13 mi), Meadow Creek to Sewell (32 mi), and Sewell to Fayette (8 mi)(Wiley, 1989).

Between Hinton and Meadow Creek, the stream width is about 850 ft, and the flood plain is primarily on one bank and is about 1,500 ft wide (discharges considered in this study do not leave the main channel in this subreach). Average depth of the river for discharges of 2,000 ft^3/s is about 5 ft, and the bed slope is about 1.5 ft per 1,000 ft. This slope includes two large falls, Brooks (an 8- to 10-ft drop) and Sandstone (about a 25-ft drop) (fig. 3). The deepest pools for discharges of 2,000 ft^3/s in this subreach are downstream from these falls and are 15 to 20 ft deep.

Between Meadow Creek and Sewell, the most apparent change in channel geometry, as compared to the Hinton-to-Meadow Creek subreach, is the lack of a wide flood plain. The average stream width in this subreach is about 550 ft, the average depth for discharges of 2,000 ft^3/s is 8 ft, and the bed slope remains unchanged from that of the Hinton-to-Meadow Creek subreach. Pool depths for discharges of 2,000 ft^3/s are 20 to 25 ft near the towns of Glade, Thurmond, and Beury (fig. 3).

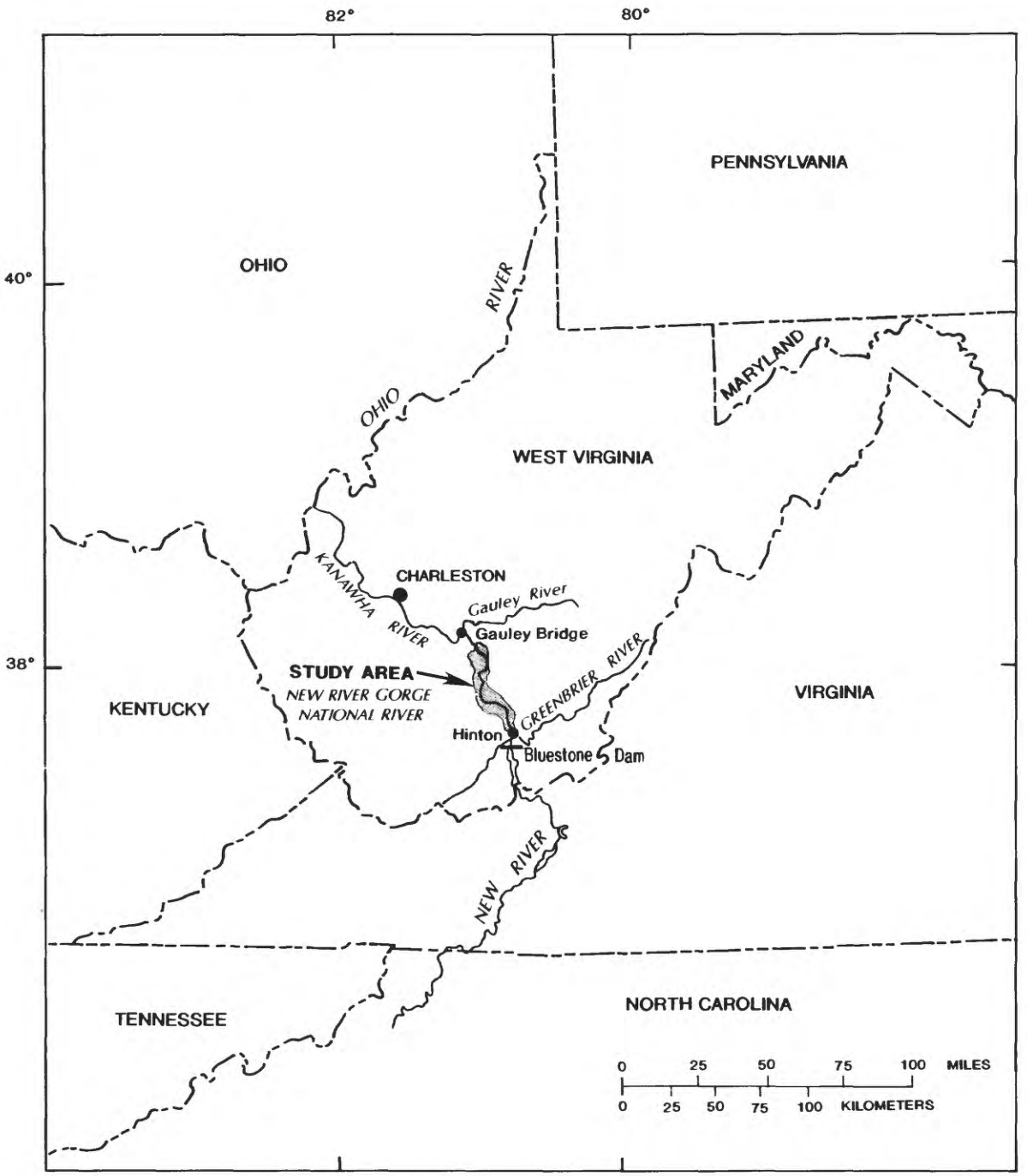

Figure 1.--Location of the New River. (Modified from Appel and Moles, 1987, p. 3.)

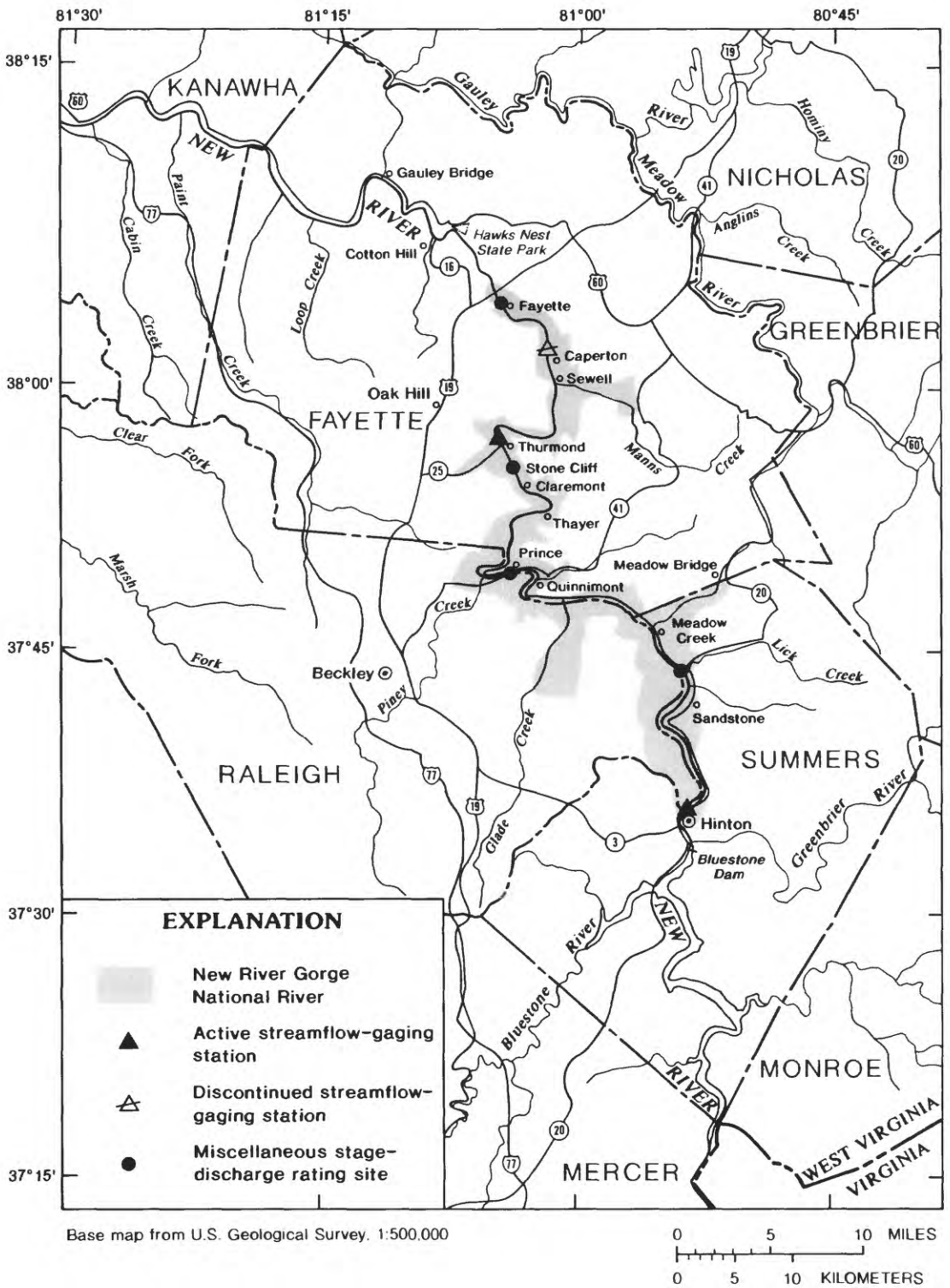

Figure 2.--Study area and New River Gorge National River.

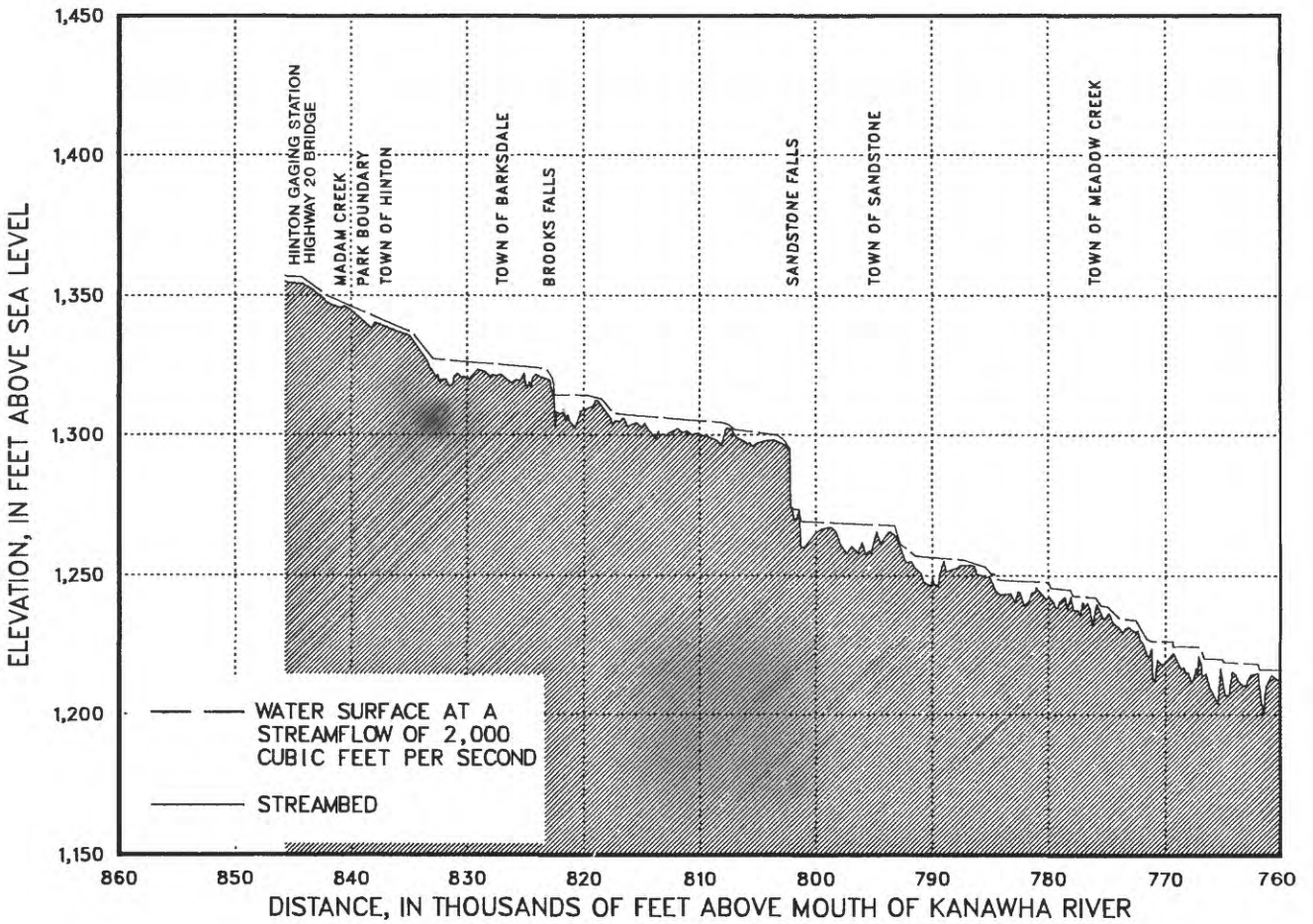

Figure 3.--Water-Surface and streambed profiles in the New River Gorge National River.

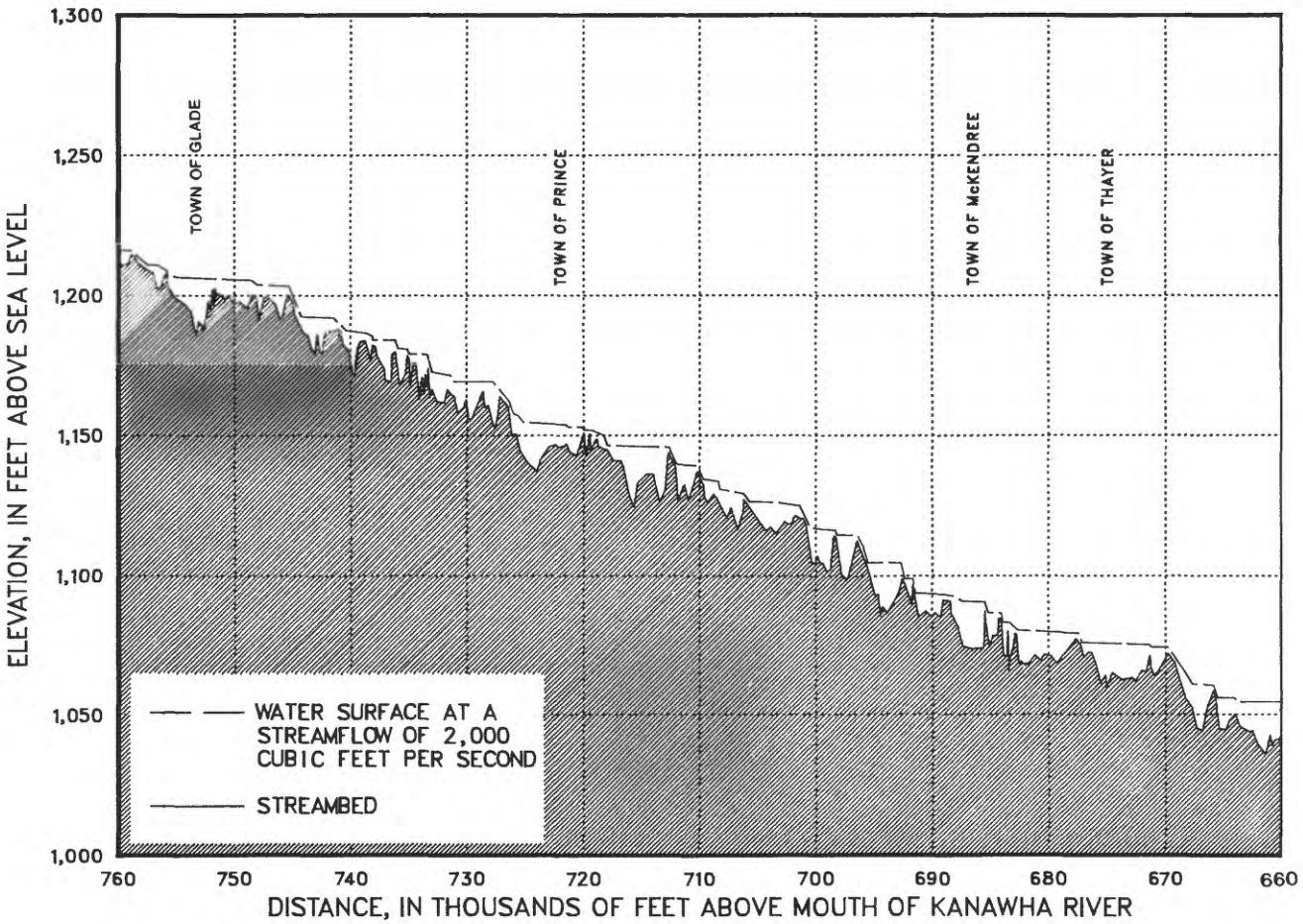

Figure 3.--Water-surface and streambed profiles in the New River Gorge National River (continued).

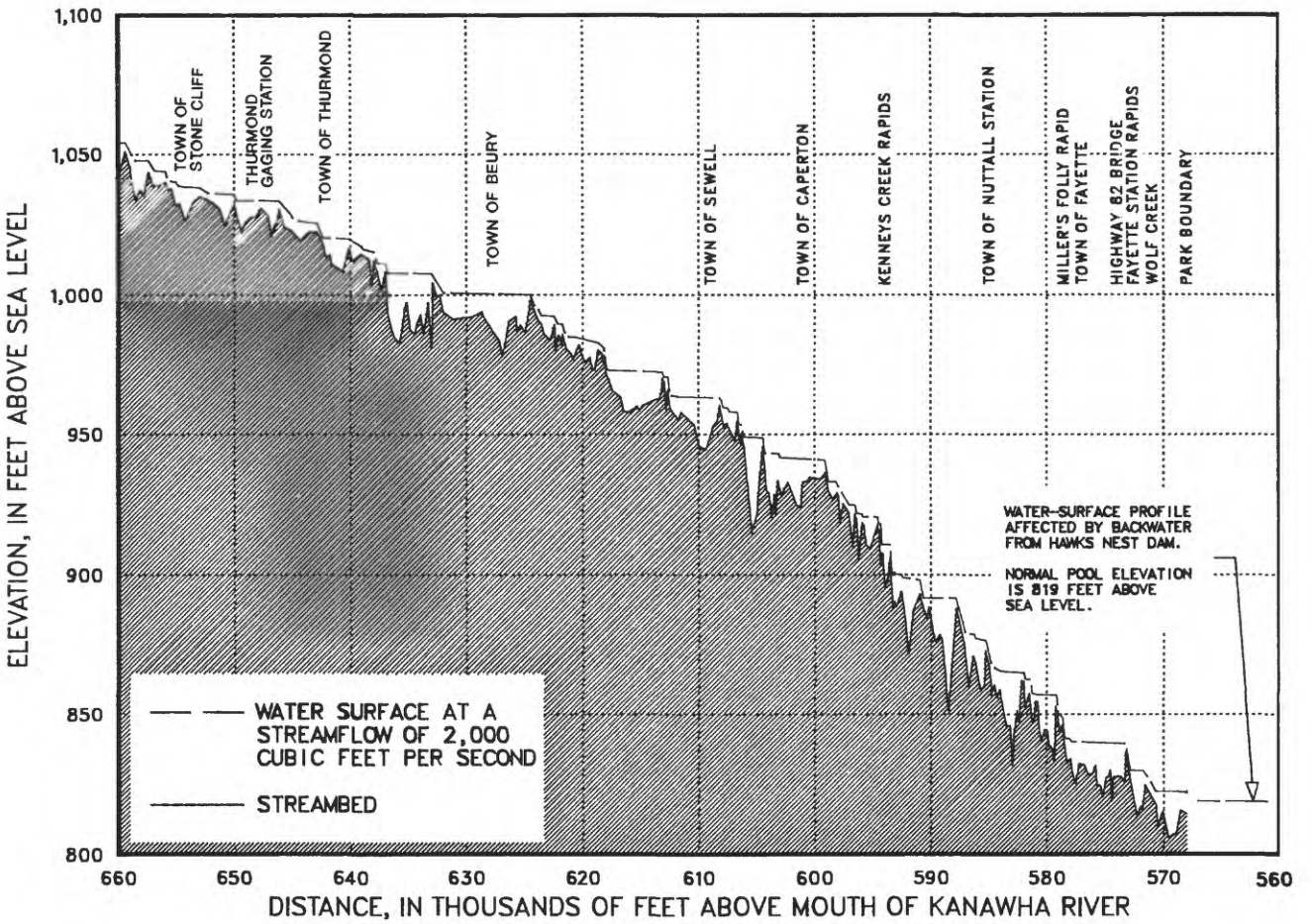

Figure 3.--Water-surface and streambed profiles in the New River Gorge National River (continued).

Between Sewell and Fayette, the most apparent changes in the river, as compared to the other subreaches, are the narrowing of the stream channel and the increasing boulder size. For a typical river cross section in this subreach, the stream width is about 350 ft, and the stream bottom is very irregular (rough). There is no flood plain because the streambanks are the valley walls. The bed slope is about 4 ft per 1,000 ft. The average depth in this subreach for discharges of 2,000 ft^3/s is about 12 ft, and the deepest pools are 35 to 40 ft deep. These pools are about 0.5 mi upstream from Caperton and near Nuttall Station.

A few small islands are scattered throughout the study reach. In all cases, there is a principal channel along one side of the island and a smaller channel along the other side. Three islands, approximately 0.8 mi, 0.4 mi, and 0.2 mi long, are in the Hinton-to-Meadow Creek subreach, and one island, approximately 0.2 mi long, is in the Meadow Creek-to-Sewell subreach. There are no islands in the Sewell-to-Fayette subreach.

FLOW AND SOLUTE-TRANSPORT MODELS

Three USGS computer models were used in this study: a steady-flow model, an unsteady-flow model, and a solute-transport model. The WSPRO (Water Surface PROfile) Fortran program is a steady-state, one-dimensional, open-channel-flow model (steady-flow model) based on the conservation of energy (Shearman and others, 1986). The DAFLOW (Diffusion Analogy FLOW) Fortran program is a one-dimensional, open-channel-flow model (unsteady-flow model) based on diffusion analogy (Jobson, 1989). The BLTM (Branch Lagrangian Transport Model) Fortran program is a one-dimensional water-quality model (solute-transport model) based on the conservation of mass (Jobson and Schoellhamer, 1987).

The steady-flow model, WSPRO, solves the energy equation between two successive cross sections for the water-surface elevation. Input data requirements include cross-section reference distances, cross-section geometry data, Manning's roughness coefficients, discharge, and starting water-surface elevation. The program offers many options, including calculating water-surface elevations through bridges and culverts; varying the Manning's roughness coefficient with hydraulic depth and subareas of cross sections; specifying flow lengths between cross sections or subareas of cross sections that override reference distances; solving the equation for critical or subcritical flows in the upstream direction and for critical or supercritical flows in the downstream direction; and providing user-defined output tables selected from more than 50 parameters and variables used in the model.

The unsteady-flow model, DAFLOW, solves the diffusion-analogy equation for unsteady discharge by means of a Lagrangian solution scheme. Input-data requirements include a power-function coefficient and exponent for the relation between area and discharge; an upstream discharge-boundary condition; a wave-dispersion coefficient; a time-step size; and a network configuration of branches, grids, and reference distances representative of the study reach. The model can simulate discharge for interconnected channels and unidirectional flow. Model outputs are discharge, area, top width, and tributary inflows at user-selected grids and time-step increments. The model also includes a plot procedure and a file containing a flow field for input into the solute-transport model, BLTM.

The solute-transport model, BLTM, solves the convective-dispersion equation using a Lagrangian reference frame. Input-data requirements include a time-step size; a network configuration of branches, grids, and reference distances representative of the study reach; a flow field containing discharge, area, top width, and tributary inflow for each grid at each time step; the upstream boundary conditions for as many as 10 constituents; and the kinetics for as many as 10 constituents. The model will simulate interconnected channels and unidirectional flow. The model computes user-selectable kinetics for several constituent combinations and can include user-defined kinetics for as many as 10 constituents. Model output consists of concentrations of each constituent at user-selected time-step increments and grid locations. Plotting procedures are available for visual inspection of model output.

Steady-Flow Model

For this study, the steady-flow model, WSPRO (Water Surface PROfile), was used to develop a relation between cross-sectional area and discharge, to determine Manning's roughness coefficients, and to balance the energy equation between cross sections. The steady-flow model was run for discharges of 2,000, 5,000, 10,000, 28,000, and 80,000 ft^3/s. This range of discharge, 2,000 to 80,000 ft^3/s, is approximately equal to the range between the 90- and 5-percent flow durations statistically determined from discharge data collected at the USGS streamflow-gaging station at Hinton since the construction of Bluestone Dam. To estimate values for zero discharge, the model was evaluated at 2.0 ft^3/s because the model does not run at zero discharge and because errors were produced at 1.0 ft^3/s. These errors were not investigated because differences between river volumes and average cross-sectional areas calculated at 1.0 and 2.0 ft^3/s are insignificant compared to the total volumes and areas. The starting elevations at the most downstream cross section were determined by means of the slope/conveyance method. Local slopes were determined from the water-surface and streambed profiles (fig. 3). The energy equation was balanced by adding cross sections to reduce conveyance ratios and to locate flows in the critical-flow regime. One-thousand and sixty-nine cross sections were used to define the geometry of the 53-mile study reach. Tabular output from the model contains the information needed to calculate the volume of water in the river. This volume is divided by the river length to calculate average cross-sectional areas that can be compared to (1) the parameter A0 (area at zero discharge) in the unsteady-flow model, and (2) the relation between area and discharge of the unsteady-flow model containing the calibration coefficient A1 (hydraulic geometry coefficient for area) and exponent A2 (hydraulic geometry exponent for area).

Cross sections for the 53-mile study reach were required for steady-flow model inputs. Estimates of ground elevations for these cross sections were evaluated by use of aerial photography, topographic maps, rating curves, and water-surface and streambed profiles (Wiley and Appel, 1989).

The NPS provided a topographic map with 20-ft contours, at a scale of 1 in. = 800 ft, compiled from photos taken when discharge was approximately 28,000 ft^3/s. The NPS also provided photographs of the study area when discharge was approximately 2,000 ft^3/s. The lower-discharge photos were overlaid onto the topographic map, and the river edges were delineated onto the contour map to provide another reference point for cross-section geometry.

Water surfaces were surveyed to sea level at various discharges less than 3,000 ft^3/s. Survey points were selected upstream and downstream from each rapid. River depths were measured by electronic soundings at various discharges less than 8,000 ft^3/s. Measuring points were selected at approximately one-third of the top width from each bank where the electronic-sounding equipment indicated a change in bed slope. Surveys and river depths were corrected by the difference between the stages when data were collected and the stages for 2,000 ft^3/s at the nearest rating location (there are three USGS streamflow-gaging stations and four miscellaneous rating sites within the study reach). River-depth curves were developed from measurements taken at one-third of the top width from each bank and were averaged to develop a final depth curve. A water-surface profile at a discharge of approximately 2,000 ft^3/s and a streambed profile were computed from the data described above (fig. 3).

Cross sections were selected at river locations where changes in channel geometry were observed on the contour map. Distances along each cross section were measured from an arbitrary point on the left bank. Elevations were determined (1) at contour-line crossings by reading directly from the map, (2) at the edges of water at a discharge of 28,000 ft^3/s by extrapolating the water-surface profile and the stage-discharge rating curves, (3) at the edges of water at a discharge of 2,000 ft^3/s by reading directly from the low-water profile, and (4) at two "underwater" points approximately one-third of the top width from each bank by reading directly from the streambed profile. These cross sections were propagated, on the basis of channel geometry, to locations where the low-water and streambed profiles change. At these locations, elevations for the low-water and streambed points were edited to create a new cross section (the right-bank and left-bank elevations of the original cross section were retained).

By means of the steady-flow model, the energy equation was balanced except where critical flows were assumed to occur at river rapids and waterfalls. At some locations, the critical flow appeared to move upstream with increasing discharges. At a given cross section, streamflow that is critical at 2,000 ft^3/s may be subcritical at 5,000 ft^3/s; yet, at the cross section immediately upstream, streamflow may be subcritical at 2,000 ft^3/s and critical at 5,000 ft^3/s.

Manning's roughness coefficient.--Steady-flow model runs for discharges of 2,000, 5,000, 10,000, 28,000, and 80,000 ft^3/s were made to route starting water elevations to the rating sites in the study reach. The roughness coefficients and associated hydraulic depths for each subreach were adjusted until the model predicted rated water-surface elevations at gaging stations and miscellaneous sites. This procedure determined the Manning's roughness coefficients for the study reach.

The Manning's roughness coefficients and associated hydraulic-depth breakpoints for each subreach are shown in table 1. The roughness coefficient varies according to hydraulic depth at each cross section for each subreach. In the Sewell-to-Fayette subreach, the roughness coefficient is 0.075 when hydraulic depth is less than or equal to 4 ft. Between hydraulic depths of 4 ft and 18 ft, the roughness varies linearly from 0.075 to 0.040. The roughness coefficient is 0.040 when hydraulic depth is greater than or equal to 18 ft.

The roughness coefficient decreases with increasing hydraulic depth. At small depths, irregularities of the channel bottom result in pronounced resistance to flow. At large depths this resistance tends to be mitigated. Roughness coefficients are greatest in the Sewell-to-Fayette subreach as compared to the other subreaches. The large boulders in this subreach would tend to increase the roughness coefficient as compared to the other subreaches containing smaller rocks. Roughness coefficients determined by application of the model seem reasonable when photographs of field conditions of subreaches of the New River are compared with photographs of field conditions at similar sites with verified roughness coefficients from Water-Supply Paper 1849 (Barnes, 1967).

Table 1.--*Summary of Manning's roughness coefficients and associated hydraulic-depth breakpoints for the study reach of the New River*

Subreach	Manning's roughness coefficient	Hydraulic-depth breakpoint, in feet
Hinton to Meadow Creek	0.030	2.0
	.025	4.0
Meadow Creek to Sewell	.040	2.0
	.030	10.0
Sewell to Fayette	.075	4.0
	.040	18.0

At islands, the principal channel was given roughness coefficients and hydraulic-depth breakpoints equivalent to those for the subreach. The smaller channel and the island subarea between channels were given various roughness coefficients and hydraulic-depth breakpoints. Roughness coefficients and hydraulic-depth breakpoints for these areas were estimated from photographs presented in Water Supply Paper 1849 (Barnes, 1967).

On flood plains in the Hinton-to-Meadow Creek subreach, roughness coefficients and hydraulic-depth breakpoints were estimated from photographs presented in Water Supply Paper 1849 (Barnes, 1967). These estimates were made to complete the cross-section data set even though streamflows will not encroach the flood plains at 80,000 ft^3/s (the maximum discharge considered in this study). There were no significant flood plains in the Meadow Creek-to-Sewell and Sewell-to-Fayette subreaches.

Rating curves.--The difference between predicted and observed water-surface elevations at the rating sites are listed in table 2. Hinton and Thurmond are operating gaging stations, Caperton is a discontinued gaging station, and the other locations listed are miscellaneous-ratings sites.

Differences between the predicted and observed water-surface elevations for the Stone Cliff and Prince sites are greater than 1 ft. Water-surface elevations at the miscellaneous sites are less accurate than measurements at the gaged sites. Miscellaneous ratings are based on two or three water-level measurements made by use of a hand-held tape. Because water surfaces were rough at the time of measurement, especially at the high discharges, less weight was given to the miscellaneous ratings when assigning roughness and hydraulic depths for each subreach during model calibration.

Table 2.--*Differences between predicted and observed water-surface elevations at rating sites used to calibrate the steady-flow model*

[ft^3/s, cubic feet per second. All differences are in feet. Positive values indicate the model predicts a higher water-surface elevation than the rated elevation. Negative values indicate the model predicts a lower water-surface elevation than the rated elevation.]

Subreach and rating site	Difference between predicted and observed elevations for a given discharge				
	2,000 ft^3/s	5,000 ft^3/s	10,000 ft^3/s	28,000 ft^3/s	80,000 ft^3/s
Hinton to Meadow Creek					
Hinton	+0.04	+0.33	+0.40	+0.73	+0.41
Sandstone	+.06	+.49	+.64	+.94	-.30
Meadow Creek to Sewell					
Prince	+.42	+.23	+.15	+1.19	+.88
Stone Cliff	+.46	+.79	+1.16	+1.67	+1.67
Thurmond	+.33	-.17	-.33	-.62	+.15
Sewell to Fayette					
Caperton	-.58	-.14	-.05	+.62	+.26
Fayette	+.52	-.02	-.15	-.15	-.77

Channel storage.--Significant channel storage is apparent in the Sewell-to-Fayette subreach. For example, between Fayette Station Rapid and Miller's Folly Rapid near Fayette, at water-surface elevations for 2,000 and 80,000 ft^3/s, the pool is 10 ft deeper at the upstream end than at the downstream end.

The volume of water in storage is calculated from the steady-flow model output. The volume of water per mile is calculated for each subreach and for the entire study reach at selected discharges. Between two cross sections, the volume is equal to the sum of each cross-sectional area times half the distance between them. The volumes are summed and divided by the length of the applicable river reach (in miles) to calculate the volume of water per mile in storage (table 3).

The steady-flow model was evaluated at 2.0 ft^3/s to generate hydraulic properties for computation of the channel storage at zero discharge listed in table 3. Zero-discharge volumes per mile in the Sewell-to-Fayette subreach are larger than volumes for the other subreaches. As discharge increases, the volume per mile in the Sewell-to-Fayette subreach approximates that of the other subreaches. This volume relation results from the narrow and deep channel characteristics of the Sewell-to-Fayette subreach as compared to the channel characteristics of the other subreaches.

Table 3.--*River volumes calculated by use of the steady-flow model*

[ft^3/s, cubic feet per second. All river volumes are in acre-foot per mile.]

River reach	River volumes for a given discharge						
	0	100 ft^3/s	1,000 ft^3/s	5,000 ft^3/s	10,000 ft^3/s	28,000 ft^3/s	80,000 ft^3/s
Hinton to Meadow Creek	72.0	82.6	137	259	356	607	1,120
Meadow Creek to Sewell	122	135	182	286	371	603	1,090
Sewell to Fayette	138	156	201	301	380	577	983
Entire study reach	112	125	174	282	370	600	1,080

Verification

At 30 random locations in the study reach, water-surface elevations calculated by the model at 2,000 ft^3/s were compared to the surveyed profile that was corrected to approximately 2,000 ft^3/s. Differences between model-computed and measured water-surface elevations were less than 1 ft. Some reasons for the differences were the following:

1. The elevation correction made to the surveyed water-surface profile by use of the nearest rating curve could have been at a location where the nearest rating curve did not accurately represent the hydraulics of the stream.
2. The discharge correction made from the traveltime of waves at the nearest USGS gaging station may not have been accurately estimated.
3. The 1-foot accuracy limit of the electronic sounding equipment may not have been sufficient, especially at low-water control cross sections.
4. Calculation of the bed elevation at cross sections from averaged depths one-third the top width from each bank may misrepresent the geometry at low-water control cross sections.

The sensitivity of the steady-flow model to Manning's roughness coefficients and the effective hydraulic-depth breakpoints associated with Manning's roughness was evaluated. Manning's roughness coefficients and hydraulic-depth breakpoints for the channel were both increased and decreased by 20 percent to compare predicted water-surface elevations at rating sites to those of the calibrated model (tables 4-7).

As Manning's roughness coefficients increase, the predicted water-surface elevations increase, and as Manning's roughness coefficients decrease, the predicted water-surface elevations decrease (tables 4 and 5). As effective hydraulic-depth breakpoints increase, the predicted water-surface elevations increase, and as effective hydraulic-depth breakpoints decrease, the predicted water-surface elevations decrease (tables 6 and 7). In both sensitivity tests, as the variable is increased, the conveyance of a cross section is reduced and a larger area is required for the same discharge; the increase of required area increases the predicted water-surface elevation. The model is more sensitive to adjustments of Manning's roughness coefficients than to adjustments of hydraulic-depth breakpoints.

The model was not subjected to a sensitivity test for the number of cross sections because a highly selective decrease in cross sections would be required to maintain a balance of the energy equation. A random reduction of cross sections would probably result in critical-flow calculations for much of the study reach, especially in the Sewell-to-Fayette subreach.

Table 4.--*Differences between predicted water-surface elevations at rating sites and those of the calibrated steady-flow model when Manning's roughness coefficients are increased by 20 percent*

[ft^3/s, cubic feet per second. All differences are in feet. Positive values indicate the model predicts a higher water- surface elevation than the calibrated elevation.]

Subreach and rating site	Difference between predicted and calibrated elevations for a given discharge				
	2,000 ft^3/s	5,000 ft^3/s	10,000 ft^3/s	28,000 ft^3/s	80,000 ft^3/s
Hinton to Meadow Creek					
Hinton	+0.18	+0.23	+0.28	+0.48	+0.77
Sandstone	+.24	+.32	+.41	+.53	+1.06
Meadow Creek to Sewell					
Prince	+.15	+.23	+.46	+.79	+1.12
Stone Cliff	+.26	+.40	+.56	+.88	+1.48
Thurmond	+.08	+.10	+.17	+.41	+.79
Sewell to Fayette					
Caperton	+.31	+.38	+.52	+.75	+1.20
Fayette	+.18	+.30	+.44	+.63	+.83

Table 5.--*Differences between predicted water-surface elevations at rating sites and those of the calibrated steady-flow model when Manning's roughness coefficients are decreased by 20 percent*

[ft^3/s, cubic feet per second. All differences are in feet. Negative values indicate the model predicts a lower water-surface elevation than the calibrated elevation.]

Subreach and rating site	Difference between predicted and calibrated elevations for a given discharge				
	2,000 ft^3/s	5,000 ft^3/s	10,000 ft^3/s	28,000 ft^3/s	80,000 ft^3/s
Hinton to Meadow Creek					
Hinton	-0.20	-0.23	-0.31	-0.50	-0.76
Sandstone	-.26	-.35	-.44	-.59	-.95
Meadow Creek to Sewell					
Prince	-.21	-.17	-.42	-.54	-.55
Stone Cliff	-.28	-.42	-.59	-.89	-1.47
Thurmond	-.06	-.09	-.13	-.19	-.37
Sewell to Fayette					
Caperton	-.38	-.43	-.56	-.77	-1.23
Fayette	-.14	-.21	-.34	-.54	-.72

Table 6.--*Differences between predicted water-surface elevations at rating sites and those of the calibrated steady-flow model when hydraulic-depth breakpoints are increased by 20 percent*

[ft^3/s, cubic feet per second. All differences are in feet.. Positive values indicate the model predicts a higher water-surface elevation than the calibrated elevation.]

Subreach and rating site	Difference between predicted and calibrated elevations for a given discharge				
	2,000 ft^3/s	5,000 ft^3/s	10,000 ft^3/s	28,000 ft^3/s	80,000 ft^3/s
Hinton to Meadow Creek					
Hinton	0.00	+0.03	+0.07	+0.04	0.00
Sandstone	+.02	+.05	+.06	.00	.00
Meadow Creek to Sewell					
Prince	.00	+.01	+.08	+.09	+.07
Stone Cliff	+.02	+.07	+.10	+.20	+.01
Thurmond	+.01	+.03	+.01	+.04	+.06
Sewell to Fayette					
Caperton	.00	+.04	+.09	+.25	+.70
Fayette	+.01	+.07	+.32	+.33	+.39

Table 7.--*Differences between predicted water-surface elevations at rating sites and those of the calibrated steady-flow model when hydraulic-depth breakpoints are decreased by 20 percent*

[ft^3/s, cubic feet per second. All differences are in feet. Negative values indicate the model predicts a lower water-surface elevation than the calibrated elevation.]

Subreach and rating site	Difference between predicted and calibrated elevations for a given discharge				
	2,000 ft^3/s	5,000 ft^3/s	10,000 ft^3/s	28,000 ft^3/s	80,000 ft^3/s
Hinton to Meadow Creek					
Hinton	0.00	-0.05	-0.09	0.00	0.00
Sandstone	-.04	-.07	-.03	.00	.00
Meadow Creek to Sewell					
Prince	-.01	-.02	-.08	-.06	-.04
Stone Cliff	-.02	-.07	-.13	-.10	-.01
Thurmond	-.01	-.02	-.02	-.04	-.02
Sewell to Fayette					
Caperton	-.04	-.05	-.13	-.34	-.50
Fayette	-.02	-.09	-.20	-.40	-.13

Unsteady-Flow Model

For this study, the unsteady-flow model, DAFLOW (Diffusion Analogy FLOW), was applied without consideration to calculated quantities from application of the steady-flow model, WSPRO. The unsteady-flow model was used to determine unsteady-flow characteristics of the study reach and to provide a flow field for the solute-transport model, BLTM (Branch Lagrangian Transport Model). A single branch with eleven grids was used to represent the study reach. Estimation equations and tables were used to determine initial model parameters, then model parameters were adjusted until simulated traveltimes of waves matched measured traveltimes. The reader is referred to the DAFLOW user's manual for additional description of parameters and their meanings (Jobson, 1989).

Calibration

The unsteady-flow model was calibrated by adjusting model parameters until the simulated traveltimes of waves matched the measured traveltimes of waves (fig. 4). These traveltimes, which represent the arrival time of the leading edge of a wave, are referenced to the discharge before the wave is produced. Figure 4 was developed in a previous study by Appel (1983). In this previous study, waves were produced by regulated releases from Bluestone Dam, and traveltimes of the leading edge of the wave were measured at locations downstream. In addition, traveltimes of selected waves recorded at continuous-record gaging stations at Hinton and Thurmond were used to develop figure 4.

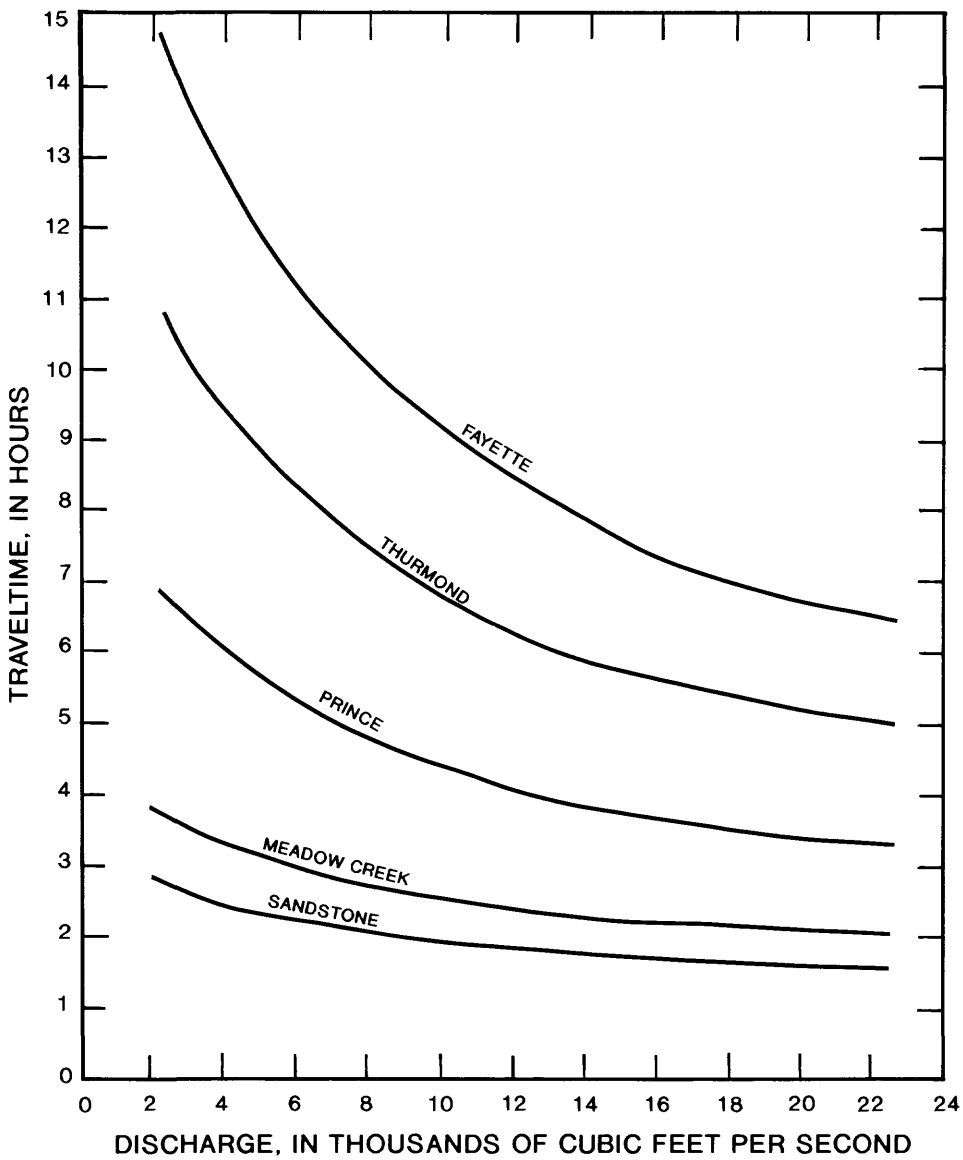

Figure 4.--Traveltimes of flood waves from Hinton to selected communities in the New River Gorge. (Modified from Appel, 1983, p. 10.)

The study reach was represented in the unsteady-flow model as a single branch with eleven grids. The location and significance of each grid is summarized in table 8. The reference distance in table 8 is equal to river distances used in the steady-flow model, except that the measurement in the steady-flow model is in feet and in the upstream direction.

Initial values for model parameters were determined by use of tabulated values and equations from the DAFLOW user's manual. Calibration parameters A2 (hydraulic geometry exponent for area) and W2 (hydraulic exponent for width) were estimated from tabulated values as 0.66 and 0.26, respectively (Jobson, 1989, p. 5). Calibration parameters A0 (average cross-sectional area at zero discharge), A1 (hydraulic geometry coefficient for area), DF (wave dispersion coefficient), and W1 (hydraulic geometry coefficient for width) were estimated by use of equations 3, 4, 11, and 13 in the user's manual (Jobson, 1989). A discussion of estimating procedures can be found on pages 24-25 of the user's manual (Jobson, 1989). Additional required information of average river slopes, river widths, and representative discharge for river widths is presented in the "Description of Study Reach" section of this report. Figure 4 of this report contains the traveltimes of waves and representative discharges necessary for making initial parameter estimates.

Table 8.--*Location and description of grids for the unsteady-flow model*

Grid number	Reference distance, in miles	Description of grid
1	0	Location of Hinton gaging station. Beginning of Hinton-to-Meadow Creek subreach.
2	9.470	Location of traveltime-of-wave site (Sandstone).
3	10.43	Location of dye-measurement site and miscellaneous rating curve (Sandstone).
4	13.07	Location of traveltime-of-wave and dye-measurement site (Meadow Creek). End of Hinton-to-Meadow Creek subreach and beginning of Meadow Creek-to-Sewell subreach.
5	23.86	Location of traveltime-of-wave and dye-measurement site, and miscellaneous rating curve (Prince).
6	36.14	Location of dye-measurement site and miscellaneous rating curve (Stone Cliff).
7	37.58	Location of Thurmond gaging station and traveltime-of-wave site.
8	44.87	End of Meadow Creek-to-Sewell subreach and beginning of Sewell-to-Fayette subreach.
9	46.44	Location of Caperton gaging station (discontinued).
10	51.36	Location of traveltime-of-wave and dye-measurement site, and miscellaneous rating curve (Fayette).
11	52.50	End of Sewell-to-Fayette subreach.

Initial flow conditions (time step zero) were set to the calibration discharge (a value from the x-axis of fig. 4), and discharge was increased and held steady at the adjusted discharge to establish a wave. The new discharge was 10 to 20 percent greater than the discharge for the initial flow condition. The irregularity of the discharge increase (10 to 20 percent) does not affect model calibration because the traveltime of the leading edge of a wave is related to discharge before the change occurs, not to the magnitude of the change. The discharge increase was rounded to the nearest 100 ft^3/s or 1,000 ft^3/s to simplify changes to the model during calibration. The model was run at a time step of 0.1 hour, and model output at the appropriate grid point was analyzed to determine the arrival time of the wave.

Several methods of model calibration involving adjustment of parameters A1 (hydraulic-geometry coefficient for area), A2 (hydraulic-geometry exponent for area), and DF (wave dispersion coefficient) were attempted to fit the simulated traveltimes to the measured traveltimes (fig. 4) for 2,200, 8,000, and 22,800 ft^3/s (H.E. Jobson, U.S. Geological Survey, written commun., 1990). Traveltimes at two of the three discharges were calibrated by adjusting A1 and A2; calibration of the traveltime for the third discharge was attempted by adjusting DF. All combinations of the above method among the three discharges failed to calibrate traveltimes from Sandstone to Prince. This method was tried again with traveltime being measured at a point above the leading edge of the wave (to increase the sensitivity of the parameter DF). This attempt also failed. The best result of these procedures was the prediction of the traveltime of waves at the third discharge to within 18 minutes of the measured traveltime at Prince. The difference between the predicted traveltime and the measured traveltime at Thurmond was greater than 1 hour. An error of greater than 1 hour was considered unacceptable in this study, and calibration at Fayette was not attempted.

Because of the calibration difficulties, it was decided to apply two models--a low-discharge model for discharges less than or equal to 8,000 ft^3/s, and a high-discharge model for discharges greater than or equal to 8,000 ft^3/s. Attempts to calibrate the low-discharge and high-discharge models by the procedures described above were unsuccessful.

The models were eventually calibrated by (1) calculating DF by use of equation 11 in the unsteady-flow user's manual (Jobson, 1989, p. 24), (2) adjusting A1 and A2 to fit exactly the traveltimes of waves at 8,000 ft^3/s, and (3) balancing the error between traveltimes at 2,200 and 4,000 ft^3/s for the low-discharge model and at 12,000 and 22,800 ft^3/s for the high-discharge model.

Parameters of the calibrated models are listed in appendixes A and B. A0, DF, W1, and W2 listed in these appendixes are estimated from tables and equations previously discussed in this section. Values of W1 and W2 do not affect calibration of the unsteady-flow model, and the effect of A0 (which will be discussed later) is minimal. A comparison between predicted and measured traveltimes used to calibrate the unsteady-flow models is given in table 9.

Table 9.--*Differences between predicted and observed traveltimes of waves used to calibrate the unsteady-flow models*

[ft^3/s, cubic feet per second. All differences are in 0.1 hour time steps. Positive values indicate the model predicts longer traveltimes of waves than the measured traveltimes. Negative values indicate the model predicts shorter traveltimes of waves than the measured traveltimes.]

Location	Difference between predicted and measured traveltimes for a given unsteady-flow model and discharge					
	Low-discharge model			High-discharge model		
	2,200 ft^3/s	4,000 ft^3/s	8,000 ft^3/s	8,000 ft^3/s	12,000 ft^3/s	22,800 ft^3/s
Sandstone	0	0	0	0	+1	-1
Meadow Creek	+1	-1	0	0	+1	-1
Prince	+3	-2	0	0	+1	-1
Thurmond	+3	-3	0	0	+2	-2
Fayette	+3	-3	0	0	+1	-1

Discharge records at the Hinton and Thurmond streamflow-gaging stations for the period December 26, 1987, 1100 hours, to January 10, 1988, 2400 hours, were compared to the results from the two unsteady-flow models for verification. Discharge during this period ranged from 2,360 to 17,900 ft^3/s at Hinton and 3,700 to 20,100 ft^3/s at Thurmond.

Discharge records at the Hinton streamflow-gaging station were input into the unsteady-flow models to predict the observed discharges at the Thurmond streamflow-gaging station. The time step used for this verification was increased from 0.1 to 0.5 hour because the longer length of time (approximately 15 days) would produce extensive output and require thousands of model iterations. Changing the time step by this magnitude did not significantly affect the model predictions of the traveltimes of waves to Thurmond. (See sensitivity tests for time step, table 18 and table 19.) The high-discharge model included data from Hinton from December 26, 1987, 0830 hours, to January 2, 1988, 0830 hours. The flow field from the output of the high-discharge unsteady-flow model was saved. Output for the last time step of the high-discharge model was used as the initial conditions for the low-discharge model. The low-discharge model was run for the remainder of the verification period. The flow field from the output of the low-discharge unsteady-flow model was appended to the flow field of the high-discharge model to create a continuous flow field for the entire period. Editing of the file was necessary to delete a time step where the high-discharge model ends and the low-discharge model begins.

Significant tributary inflows needed to be accounted for in the verification period. This was apparent because the recorded peak discharge at Hinton was 17,900 ft^3/s and the recorded peak discharge at Thurmond was 20,100 ft^3/s for this period. A plot of observed discharges as a function of time for both streamflow-gaging stations was used to estimate an inflow hydrograph. The estimated inflow was introduced into the model at the Thurmond gaging-station grid. Because all inflow was not at this location, some accuracy was lost. Applying parts of inflow at different grids upstream based on the location of stream inflows could increase model accuracy; however, this was not done because there were several tributaries (see "Description of Study Reach") and because determination of the magnitude and traveltime of waves to produce the resultant tributary inflow hydrograph at Thurmond would have been a major task.

The predicted, observed, and inflow hydrographs at Thurmond are shown in figure 5. The loss of accuracy near the end of the verification period (where discharges are less than approximately 3,000 ft^3/s) is partly related to the procedure used to apply inflow, as described above. The inflow is large enough to alter the prediction of traveltime of the wave because the inflow is applied at the Thurmond grid instead of at grids upstream.

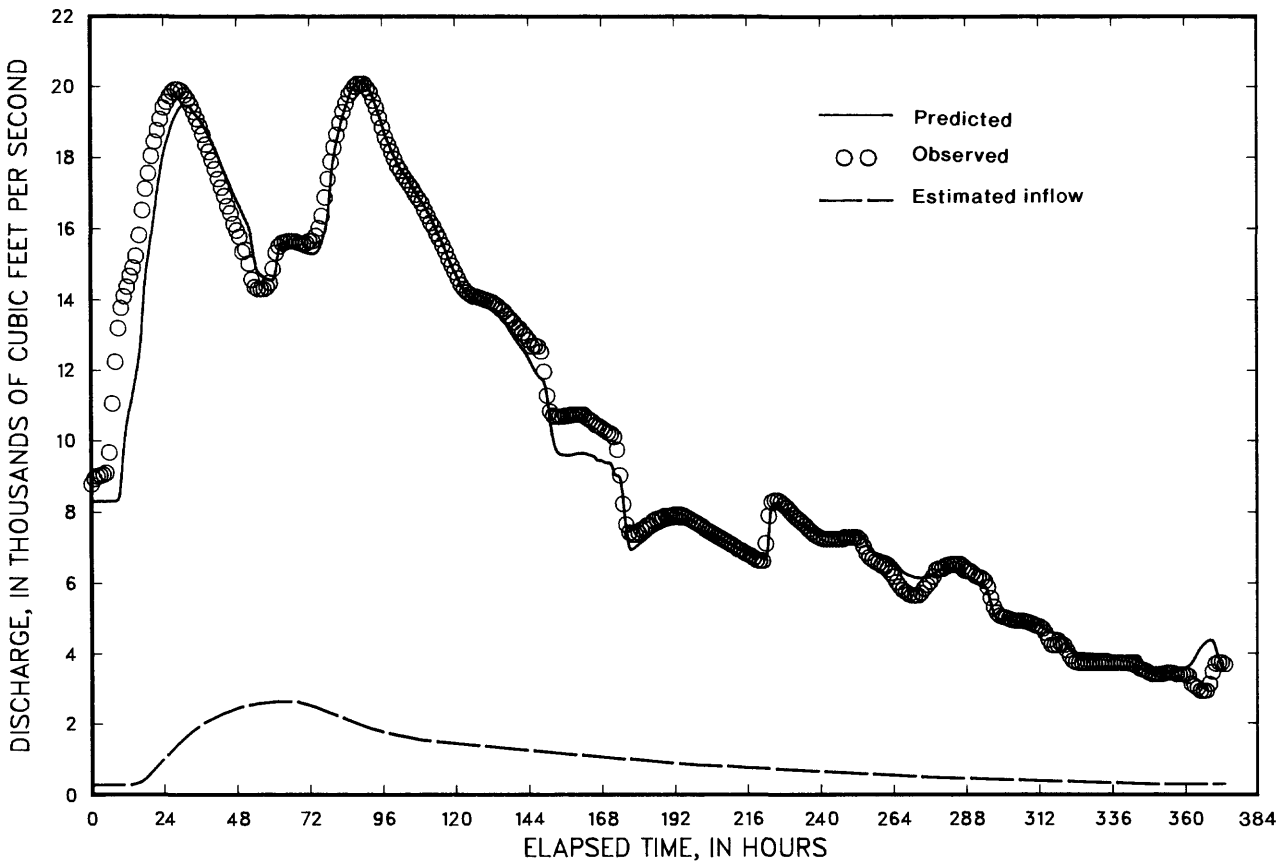

Figure 5.--Predicted, observed, and estimated-inflow discharges at Thurmond, December 26, 1987, through January 2, 1988.

The parameters A0, A1, A2, and DF were increased and decreased by 20 percent (tables 10-17) and time steps were increased by 100 percent and decreased by 50 percent (tables 18 and 19) to study sensitivity of the unsteady-flow model. During calibration, it was found that adjustment of A0 affected the traveltime of waves. The sensitivity to A0 was caused by placement of the first shock at the upstream end of the model reach (H.E. Jobson, U.S. Geological Survey, oral commun., 1990). The shock-placement step involves equation 3 in the user's manual (Jobson, 1989, p. 3). This equation was also used in the wave-dispersion step (after the first shock is placed); however, A0 "falls out" of this solution procedure and makes the model nonsensitive in the wave-dispersion step. The model was sensitive to adjustments of A0 in the shock-placement step but not in the wave-dispersion step.

The sensitivity due to increasing and decreasing A0 by 20 percent is shown in tables 10 and 11. The effects are relatively small as compared to the effects of adjustments of the other parameters. In fact, increases and decreases in A0 do not result in definite increases or decreases in the traveltime of waves.

As A1 increases, the traveltime of waves increases, and as A1 decreases, the traveltime of waves decreases (tables 12 and 13). The magnitudes of differences in the traveltimes of waves are approximately the same for increases and decreases in A1. The differences in traveltime accumulate in the downstream direction. The models are more sensitive to adjustment of A1 at lower discharges than at higher discharges.

As A2 increases, the traveltime of waves increases, and as A2 decreases, the traveltime of waves decreases (tables 14 and 15). Unlike A1, however, the magnitude of the differences in the traveltimes of waves are greater for increases in A2 than for decreases in A2. The model is more sensitive to increases in A2 than to decreases in A2 because A2 is an exponent of the relation between area and discharge (Jobson, 1989, page 3). The models are more sensitive to adjustments in A2 at high discharges than at low discharges. The differences between predicted and calibrated traveltimes of waves accumulate in the downstream direction. Table 14 is incomplete because the models were not run the necessary number of time steps to predict traveltimes of waves caused by increasing A2 by 20 percent. The models were not run additional time steps because patterns were apparent from executing the existing number of time steps and because altering the input file for additional time steps was time consuming.

Generally, as DF increases, the traveltime of waves decreases, and as DF decreases, the traveltime of waves increases (tables 16 and 17); however, this relation does not hold true for all cases. Output from the low-discharge unsteady-flow model shows an opposite trend in the downstream subreaches at Thurmond and Fayette when DF is decreased (table 17) and also at Fayette when DF is increased (table 16). Why this opposite trend is present is not understood, but the change in the relation of DF to traveltime may be one reason that the unsteady-flow model could not be calibrated through the entire range of discharge.

No general trend in the traveltime of waves was established by increasing and decreasing time steps (tables 18 and 19). The low-discharge unsteady-flow model appears to show a sensitivity similar to that caused by adjustments in DF at Thurmond and Fayette. At 2,200 and 8,000 ft^3/s, the traveltime of waves decreases with an increase in time step, and the traveltime of waves increases with the decrease in time step. This trend at 2,200 and 8,000 ft^3/s is not understood.

In general, the unsteady-flow models are least sensitive to adjustments in A0 and time step, more sensitive to adjustments in A1, and most sensitive to adjustments in A2. The sensitivity at 2,200 and 8,000 ft^3/s to changes in DF and time step cannot be explained.

Table 10.--*Differences between predicted traveltimes of waves and those of the calibrated unsteady-flow models when average cross-sectional area of zero flow (A0) is increased by 20 percent*

[ft^3/s, cubic feet per second. All differences are in 0.1 hour time steps. Positive values indicate the model predicts longer traveltimes of waves than the calibrated traveltimes. Negative values indicate the model predicts shorter traveltimes of waves than the calibrated traveltimes.]

Location	Difference between predicted and calibrated traveltimes for a given unsteady-flow model and discharge					
	Low-discharge model			High-discharge model		
	2,200 ft^3/s	4,000 ft^3/s	8,000 ft^3/s	8,000 ft^3/s	12,000 ft^3/s	22,800 ft^3/s
Sandstone	0	-1	-1	0	0	0
Meadow Creek	0	0	0	+1	+1	0
Prince	0	0	0	0	0	0
Thurmond	-1	-1	+1	-1	0	0
Fayette	0	-2	0	0	0	-1

Table 11.--*Differences between predicted traveltimes of waves and those of the calibrated unsteady-flow models when average cross-sectional area of zero flow (A0) is decreased by 20 percent*

[ft^3/s, cubic feet per second. All differences are in 0.1 hour time steps. Positive values indicate the model predicts longer traveltimes of waves than the calibrated traveltimes. Negative values indicate the model predicts shorter traveltimes of waves than the calibrated traveltimes.]

Location	Difference between predicted and calibrated traveltimes for a given unsteady-flow model and discharge					
	Low-discharge model			High-discharge model		
	2,200 ft^3/s	4,000 ft^3/s	8,000 ft^3/s	8,000 ft^3/s	12,000 ft^3/s	22,800 ft^3/s
Sandstone	0	-1	0	0	0	0
Meadow Creek	0	0	0	0	+1	0
Prince	0	0	+1	0	0	0
Thurmond	0	0	0	-1	0	0
Fayette	+1	-1	0	0	0	-1

Table 12.--*Differences between predicted traveltimes of waves and those of the calibrated unsteady-flow models when hydraulic geometry coefficient for area (A1) is increased by 20 percent*

[ft^3/s, cubic feet per second. All differences are in 0.1 hour time steps. Positive values indicate the model predicts longer traveltimes of waves than the calibrated traveltimes.]

Location	Difference between predicted and calibrated traveltimes for a given unsteady-flow model and discharge					
	Low-discharge model			High-discharge model		
	2,200 ft^3/s	4,000 ft^3/s	8,000 ft^3/s	8,000 ft^3/s	12,000 ft^3/s	22,800 ft^3/s
Sandstone	+5	+3	+3	+3	+3	+2
Meadow Creek	+7	+6	+4	+5	+5	+3
Prince	+12	+10	+9	+7	+7	+5
Thurmond	+19	+17	+14	+12	+12	+9
Fayette	+28	+22	+21	+17	+16	+11

Table 13.--*Differences between predicted traveltimes of waves and those of the calibrated unsteady-flow models when hydraulic geometry coefficient for area (A1) is decreased by 20 percent*

[ft^3/s, cubic feet per second. All differences are in 0.1 hour time steps. Negative values indicate the model predicts shorter traveltimes of waves than the calibrated traveltimes.]

Location	Difference between predicted and calibrated traveltimes for a given unsteady-flow model and discharge					
	Low-discharge model			High-discharge model		
	2,200 ft^3/s	4,000 ft^3/s	8,000 ft^3/s	8,000 ft^3/s	12,000 ft^3/s	22,800 ft^3/s
Sandstone	-5	-4	-4	-3	-3	-2
Meadow Creek	-7	-6	-5	-4	-4	-4
Prince	-13	-11	-11	-8	-7	-6
Thurmond	-21	-17	-20	-14	-11	-10
Fayette	-29	-26	-29	-19	-16	-14

Table 14.--*Differences between predicted traveltimes of waves and those of the calibrated unsteady-flow models when hydraulic geometry exponent for area (A2) is increased by 20 percent*

[ft^3/s, cubic feet per second. All differences are in 0.1 hour time steps. Positive values indicate the model predicts longer traveltimes of waves than the calibrated traveltimes.]

Location	Difference between predicted and calibrated traveltimes for a given unsteady-flow model and discharge					
	Low-discharge model			High-discharge model		
	2,200 ft^3/s	4,000 ft^3/s	8,000 ft^3/s	8,000 ft^3/s	12,000 ft^3/s	22,800 ft^3/s
Sandstone	+55	+46	+48	+23	+26	+25
Meadow Creek	+79	+72	+74	+32	+33	+29
Prince	(1)	(1)	+122	+63	+66	+55
Thurmond	(1)	(1)	(1)	(1)	+103	+88
Fayette	(1)	(1)	(1)	(1)	(1)	(1)

[1] Value is greater than the number of time steps used in the model.

Table 15.--*Differences between predicted traveltimes of waves and those of the calibrated unsteady-flow models when hydraulic geometry exponent for area (A2) is decreased by 20 percent*

[ft^3/s, cubic feet per second. All differences are in 0.1 hour time steps. Negative values indicate the model predicts shorter traveltimes of waves than the calibrated traveltimes.]

Location	Difference between predicted and calibrated traveltimes for a given unsteady-flow model and discharge					
	Low-discharge model			High-discharge model		
	2,200 ft^3/s	4,000 ft^3/s	8,000 ft^3/s	8,000 ft^3/s	12,000 ft^3/s	22,800 ft^3/s
Sandstone	-20	-18	-16	-13	-12	-10
Meadow Creek	-28	-24	-22	-16	-15	-13
Prince	-51	-42	-36	-30	-27	-22
Thurmond	-81	-67	-57	-49	-43	-33
Fayette	-110	-93	-76	-67	-57	-44

Table 16.--*Differences between predicted traveltimes of waves and those of the calibrated unsteady-flow models when the wave-dispersion coefficient (DF) is increased by 20 percent*

[ft^3/s, cubic feet per second. All differences are in 0.1 hour time steps. Positive values indicate the model predicts longer traveltimes of waves than the calibrated traveltimes. Negative values indicate the model predicts shorter traveltimes of waves than the calibrated traveltimes.]

Location	Difference between predicted and calibrated traveltimes for a given unsteady-flow model and discharge					
	Low-discharge model			High-discharge model		
	2,200 ft^3/s	4,000 ft^3/s	8,000 ft^3/s	8,000 ft^3/s	12,000 ft^3/s	22,800 ft^3/s
Sandstone	-1	-1	-1	-2	0	-1
Meadow Creek	-1	-1	-1	-1	0	-1
Prince	-2	-2	-1	-1	-1	-1
Thurmond	-2	-2	-1	-2	-1	-1
Fayette	-1	-2	+1	-3	-2	-2

Table 17.--*Differences between predicted traveltimes of waves and those of the calibrated unsteady-flow models when the wave-dispersion coefficient (DF) is decreased by 20 percent*

[ft^3/s, cubic feet per second. All differences are in 0.1 hour time steps. Positive values indicate the model predicts longer traveltimes of waves than the calibrated traveltimes. Negative values indicate the model predicts shorter traveltimes of waves than the calibrated traveltimes.]

Location	Difference between predicted and calibrated traveltimes for a given unsteady-flow model and discharge					
	Low-discharge model			High-discharge model		
	2,200 ft^3/s	4,000 ft^3/s	8,000 ft^3/s	8,000 ft^3/s	12,000 ft^3/s	22,800 ft^3/s
Sandstone	+1	+1	+1	+1	+1	+1
Meadow Creek	+1	+1	0	+2	+2	+2
Prince	+2	+1	+2	+2	+2	+1
Thurmond	+2	+2	-3	+2	+2	+1
Fayette	+4	+1	-6	+3	+1	0

Table 18.--*Differences between predicted traveltimes of waves and those of the calibrated unsteady-flow models when time step is increased by 100 percent*

[ft^3/s, cubic feet per second. All differences are in 0.1 hour time steps. Negative values indicate the model predicts shorter traveltimes of waves than the calibrated traveltimes.]

Location	Difference between predicted and calibrated traveltimes for a given unsteady-flow model and discharge					
	Low-discharge model			High-discharge model		
	2,200 ft^3/s	4,000 ft^3/s	8,000 ft^3/s	8,000 ft^3/s	12,000 ft^3/s	22,800 ft^3/s
Sandstone	0	0	0	0	0	0
Meadow Creek	0	0	0	0	0	0
Prince	0	0	-2	0	0	0
Thurmond	0	0	-4	0	-1	0
Fayette	-2	-2	-5	-1	-2	-1

Table 19.--*Differences between predicted traveltimes of waves and those of the calibrated unsteady-flow models when time step is decreased by 50 percent*

[ft^3/s, cubic feet per second. All differences are in 0.1 hour time steps. Positive values indicate the model predicts longer traveltimes of waves than the calibrated traveltimes. Negative values indicate the model predicts shorter traveltimes of waves than the calibrated traveltimes.]

Location	Difference between predicted and calibrated traveltimes for a given unsteady-flow model and discharge					
	Low-discharge model			High-discharge model		
	2,200 ft^3/s	4,000 ft^3/s	8,000 ft^3/s	8,000 ft^3/s	12,000 ft^3/s	22,800 ft^3/s
Sandstone	+2	-1	-1	+1	+1	0
Meadow Creek	+2	0	0	+1	+1	-1
Prince	0	0	+1	+1	+1	0
Thurmond	+2	+1	+1	0	+3	+1
Fayette	+4	0	+4	0	+1	-1

Solute-Transport Model

For this study, the solute-transport model, BLTM (Branch Lagrangian Transport Model), was applied to the study reach to track the transport of a suspended solute by selecting kinetics for a conservative solute (dye). Estimating equations were used to determine initial conditions. Changes in channel characteristics were defined by 3 branches and 13 grids. The parameter A0, an unsteady-flow model parameter, is adjusted to calibrate the traveltime of peak concentration in the solute-transport model (this flow parameter does not significantly affect discharge calculations by the unsteady-flow model). The flow fields used with the solute-transport models were supplied by two (high-discharge and low-discharge) unsteady-flow models. Because the solute-transport model does not allow for multiple flow fields describing the flow characteristics of the same branch, two solute-transport models were developed. The reader is referred to the solute-transport model user's manual for additional definition and description of parameters (Jobson and Schoellhamer, 1987).

Calibration

Two solute-transport models--high-discharge and low-discharge--were calibrated by adjusting model parameters until the simulated peak concentrations and the traveltimes of peak concentrations matched the peak concentrations and the traveltimes of peak concentrations from figures 6 and 7. These figures were developed in a previous study by Appel and Moles (1987).

The study subreaches--Hinton to Meadow Creek, Meadow Creek to Sewell, and Sewell to Fayette--were represented by the models as three branches. The flow fields from the unsteady-flow models were easily modified from one branch to three; however, the unsteady-flow models were still run as a single branch. Flow-field modifications involved (1) renumbering of branches and grids and (2) copying flow characteristics at junctions between branches to obtain flow characteristics for each grid of each branch. Thirteen grids (including two grids copied at junctions between branches) and three branches represented the study reach for application of the solute-transport model.

The parameters A0 (average cross-sectional area of zero discharge), W1 (hydraulic geometry coefficient for width), and W2 (hydraulic geometry exponent for width) in the unsteady-flow model affect calculations of the solute-transport model. Initial conditions for these parameters were discussed previously in the "Unsteady-Flow Model" section of this report. For this application of the solute-transport model, parameters W1 and W2 had no effect because decay subroutines that use these parameters were not necessary for predicting a conservative solute. Parameter A0 had a minimal effect in the unsteady-flow model (tables 10 and 11), but it significantly affected the traveltime of peak concentration in the solute-transport model. The solute-transport model parameter DQQ (dispersion factor) was estimated to be 0.75 from inspection of other model-simulation examples.

A concentration curve must be input into the model at the most upstream grid. The most upstream grid is at Hinton, but no dye measurement was made at this location. The most upstream dye-measurement site was at Sandstone. Because Sandstone is near the downstream end of the Hinton-to-Meadow Creek subreach, the concentration curve measured at Sandstone could be applied at Hinton. This procedure was acceptable because the hydraulics that affected the solute cloud were repeated and should not affect A0 or DQQ calibration parameters. The input concentration curves for each calibration discharge were developed from (1) traveltimes of the leading edge, the peak concentration, and the trailing edge, and (2) peak concentrations of a 20-pound slug injection predicted at Sandstone (figs. 6 and 7, and others developed by Appel and Moles, 1987, p. 13 and p. 15).

High-discharge and low-discharge steady-flow models, and high-discharge and low-discharge solute-transport models were run at a time step of 0.2 hour. This increase in time step for the unsteady-flow models did not significantly affect the predicted traveltimes of waves (tables 18 and 19). The unsteady-flow models were run for steady discharges of 3,000, 5,000, 10,000, and 22,800 ft^3/s. The solute-transport model was run such that the peak concentration of the input-concentration curve occurred at 6.2 hours.

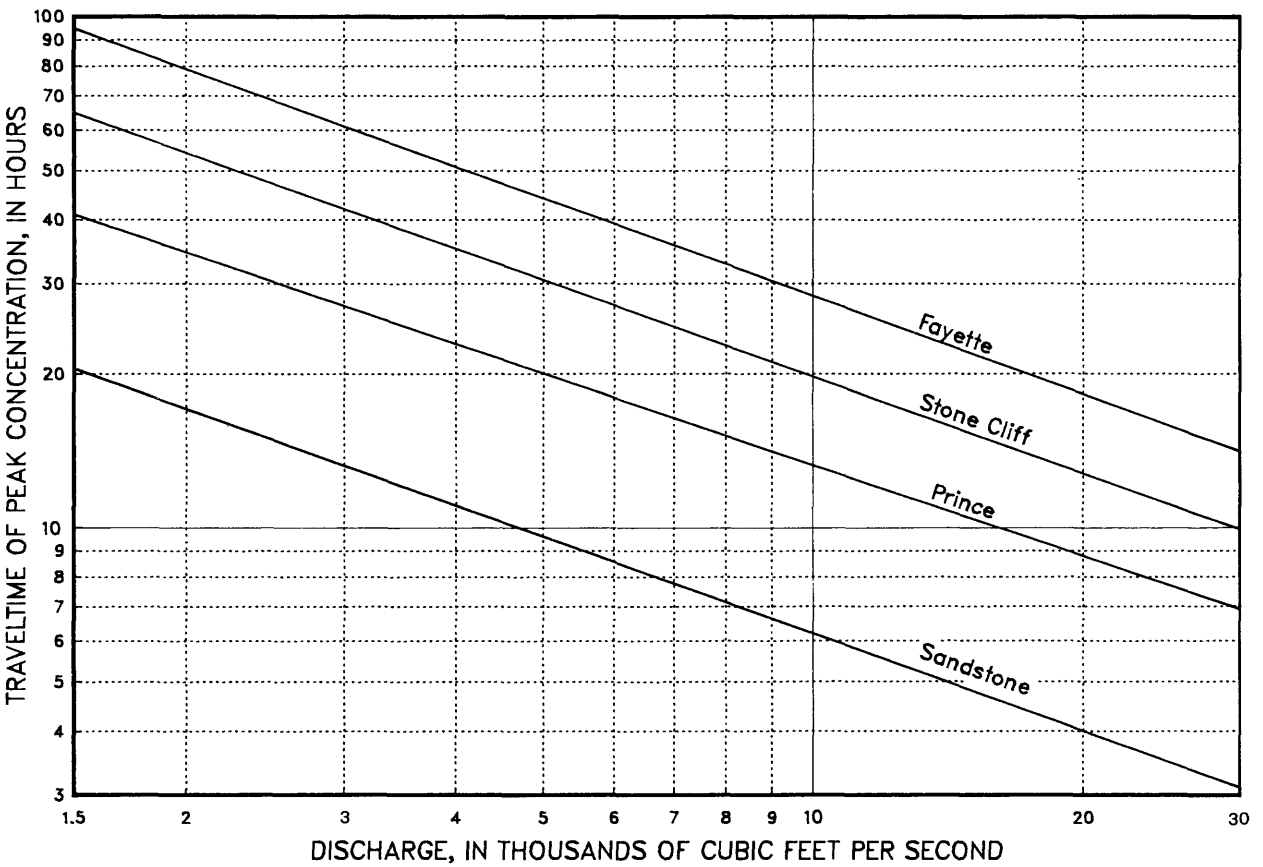

Figure 6.--Relations between discharge and the traveltime of peak concentrations of dye from Hinton to selected communities in the New River Gorge.
(Modified from Appel and Moles, 1987, p. 14.)

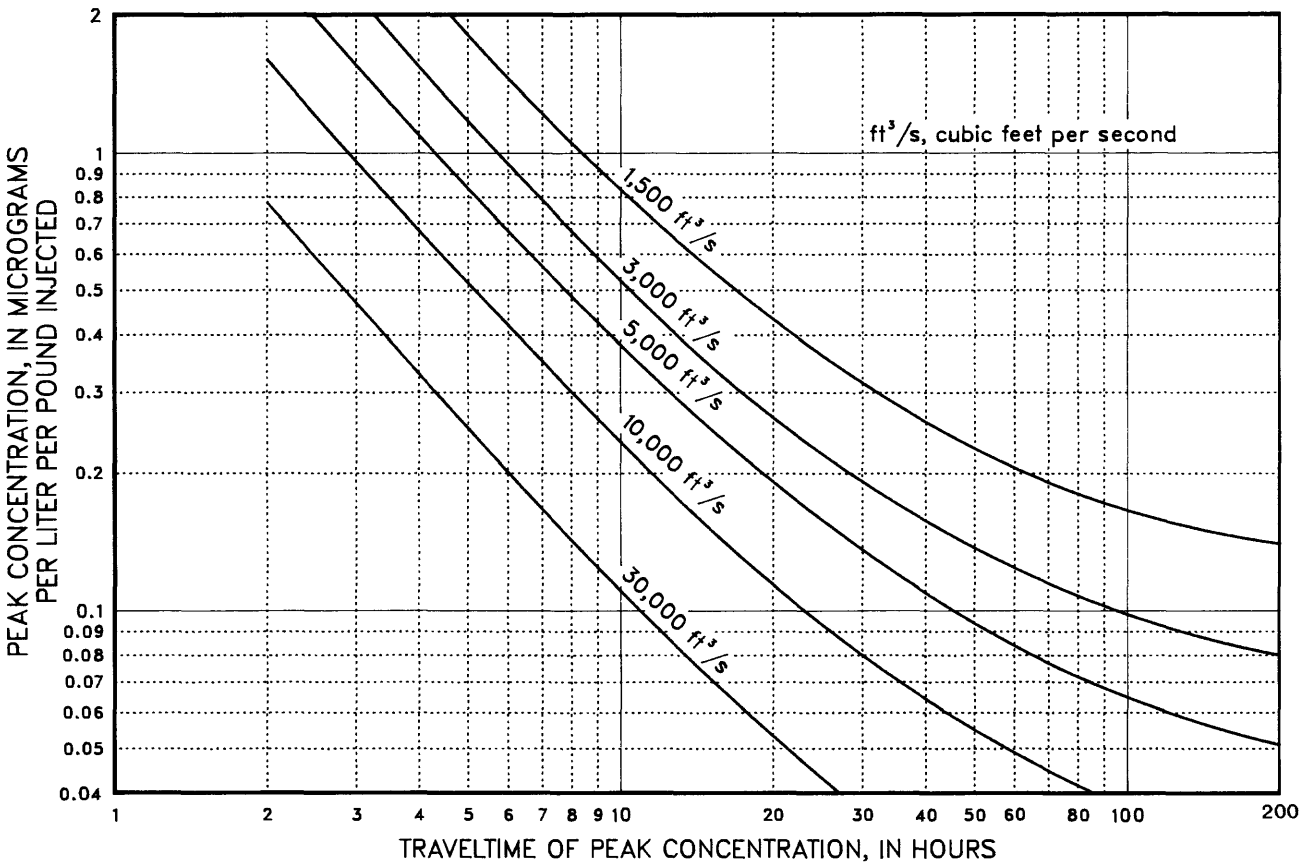

Figure 7.--Peak concentrations resulting from the injection of 1 pound of a conservative soluble material at selected discharges.(Modified from Appel and Moles, 1987, p. 19.)

For the high-discharge solute-transport model (discharges greater than or equal to 8,000 ft^3/s), measured and predicted peak concentrations and traveltimes of peak concentrations were balanced between steady discharges of 10,000 and 22,800 ft^3/s. Between Hinton and Sandstone, for calibration of 22,800 ft^3/s, A0 was reduced to zero, and the predicted traveltime of peak concentration was more than 1 hour later than the measured traveltime. Similarly, the 10,000 ft^3/s calibration predicted a later traveltime of peak concentration, but the difference from the measured traveltime was smaller. The value of A0 would have to be reduced further to decrease the difference between measured and predicted traveltimes of peak concentrations. The model could not be calibrated between Hinton and Sandstone because it was not feasible for the average cross-sectional area of zero discharge (A0) to be less than zero. The value of A0 computed for initial conditions was used between Hinton and Sandstone, and corrections to the traveltime of peak concentration were applied to calibrate the remaining study reach. DQQ was adjusted to calibrate the peak concentrations.

For the low-discharge solute-transport model (discharges less than or equal to 8,000 ft^3/s), the measured and the predicted peak concentrations and traveltimes of peak concentrations were balanced between 3,000 and 5,000 ft^3/s. The value of A0 computed for initial conditions was used between Hinton and Sandstone to avoid problems encountered in calibrating the high-discharge solute-transport model. Corrections to the traveltimes of peak concentrations were applied to calibrate the rest of the study reach. DQQ was adjusted to calibrate the peak concentrations.

The difference between measured and predicted peak concentrations and traveltimes of peak concentrations used to calibrate the low-discharge and high-discharge solute-transport models are shown in table 20. For the high-discharge solute-transport model, a partial listing of the input file containing transport parameters (including DQQ) is given in appendix C, and a partial listing of the input file containing flow-parameters (including A0, W1, and W2) is given in appendix D. For the low-discharge solute-transport model, a partial listing of the input file containing transport parameters is given in appendix E, and a partial listing of the input file containing flow parameters is given in appendix F.

Table 20.--*Differences between predicted and observed peak concentrations and between predicted and observed traveltimes of peak concentrations used to calibrate the solute-transport models*

[TT, the traveltime of peak concentration. PC, peak concentration. ft^3/s, cubic feet per second. All differences in peak concentration are in percent. All differences in traveltime are in 0.2 hour time step. Positive values indicate the model predicts a higher peak concentration or traveltime of peak concentration than the measured concentration or traveltime. Negative values indicate the model predicts a lower peak concentration or traveltime of peak concentration than the measured concentration or traveltime.]

Location	Difference in peak concentration and traveltime for a given solute-transport model and discharge							
	Low-discharge model				High-discharge model			
	3,000 ft^3/s		5,000 ft^3/s		10,000 ft^3/s		22,800 ft^3/s	
	TT	PC	TT	PC	TT	PC	TT	PC
Sandstone	[1]-16	[1]+13	[1]-11	[1]-9	[1]+11	[1]+3	[1]+8	[1]-3
Prince	+4	+6	-2	-14	+1	-10	0	+10
Stone Cliff	+5	+7	-5	-9	-2	-12	-2	+21
Fayette	+5	+14	-5	-6	0	-7	-2	+38

[1] A correction for this difference is applied to calibrate at other locations.

Two unsteady-flow dye measurements (Appel, 1987, and Wiley and Appel, 1989) and one steady-flow dye measurement (Appel and Moles, 1987) were used to verify results of the solute-transport model simulations. The flow field produced by the unsteady-flow models were modified into three branches, as in the calibration of the solute-transport models, except for the location of the first grid point of the first branch. Instead of starting at Hinton, the first grid was placed at Sandstone. The river reach between Hinton and Sandstone was not verified. The observed dye-concentration curve at Sandstone was input into the model beginning at the time step equal to the time since the slug injection. The unsteady-flow model was run with appropriate discharges, and output was modified to meet the input requirements of a three-branch solute-transport model that begins at Sandstone.

Decreasing unsteady flow.--The predicted and observed traveltimes and concentrations for decreasing unsteady flow (fig. 8) were verified as follows:

1. The high-discharge unsteady-flow model was run at a steady discharge of 8,100 ft^3/s for 9.0 hours.

2. The discharge was reduced to 8,000 ft^3/s from 9.0 to 9.2 hours.

3. Output from the high-discharge unsteady-flow model was used for initial conditions of the low-discharge unsteady-flow model.

4. The low-discharge model was run for 1.0 hour as discharge was reduced from 8,000 to 4,500 ft^3/s and then was continued at a steady discharge for the remaining time steps.

5. Output from the two unsteady-flow models were combined into one flow field, and the flow field was then modified to be one of three branches with the first grid at Sandstone.

6. The low-discharge solute-transport model was run.

The high-discharge solute-transport model was not used, although some discharges exceeded 8,000 ft^3/s. Predictions from the low-discharge solute-transport model were used because transition from the high-discharge model to the low-discharge model (that is, stopping and starting the solute-transport model) would cause locations and concentrations of parcels to be lost.

Increasing unsteady flow.--The predicted and observed traveltimes and concentrations for increasing unsteady flow (fig. 9) were verified as follows:

1. The low-discharge unsteady-flow model was run at a steady discharge of 4,500 ft^3/s for 18.0 hours.

2. The discharge was increased to 8,000 ft^3/s from 18.0 to 19.6 hours.

3. Output from the low-discharge unsteady-flow model was used for initial conditions of the high-discharge unsteady-flow model.

4. The high-discharge model was run for 1.4 hours as discharge was increased from 8,000 to 11,200 ft^3/s and then was continued at a steady discharge for the remaining time steps.

5. Output from the two unsteady-flow models were combined into one flow field, and the flow field was modified to be one of three branches with the first grid at Sandstone.

6. The low-discharge solute-transport model was run.

Again, the high-discharge solute-transport model was not used because of the high-discharge/low-discharge transition problems that occur when the solute-transport model is stopped and then started again. The initial low-discharge solute-transport model output predicted the traveltime of peak concentration at Prince approximately 2 hours sooner than the observed traveltime, and the traveltime of waves predicted by the unsteady-flow model reached Prince before the peak concentration predicted by the solute-transport model. A review of the dye measurement records showed that the initial discharge should have been 4,000 ft^3/s, not 4,500 ft^3/s. Once this correction was made, verification was successful (fig. 9).

Steady flow.--The predicted and observed peak concentrations and traveltimes of peak concentrations for a steady-flow dye measurement at 9,200 ft^3/s (fig. 10) were verified as follows:

1. The high-discharge unsteady-flow model was run at a steady discharge of 9,200 ft^3/s for all time steps.

2. Output from the high-discharge model was modified to a flow field of three branches with the first grid at Sandstone.

3. The high-discharge solute-transport model was run.

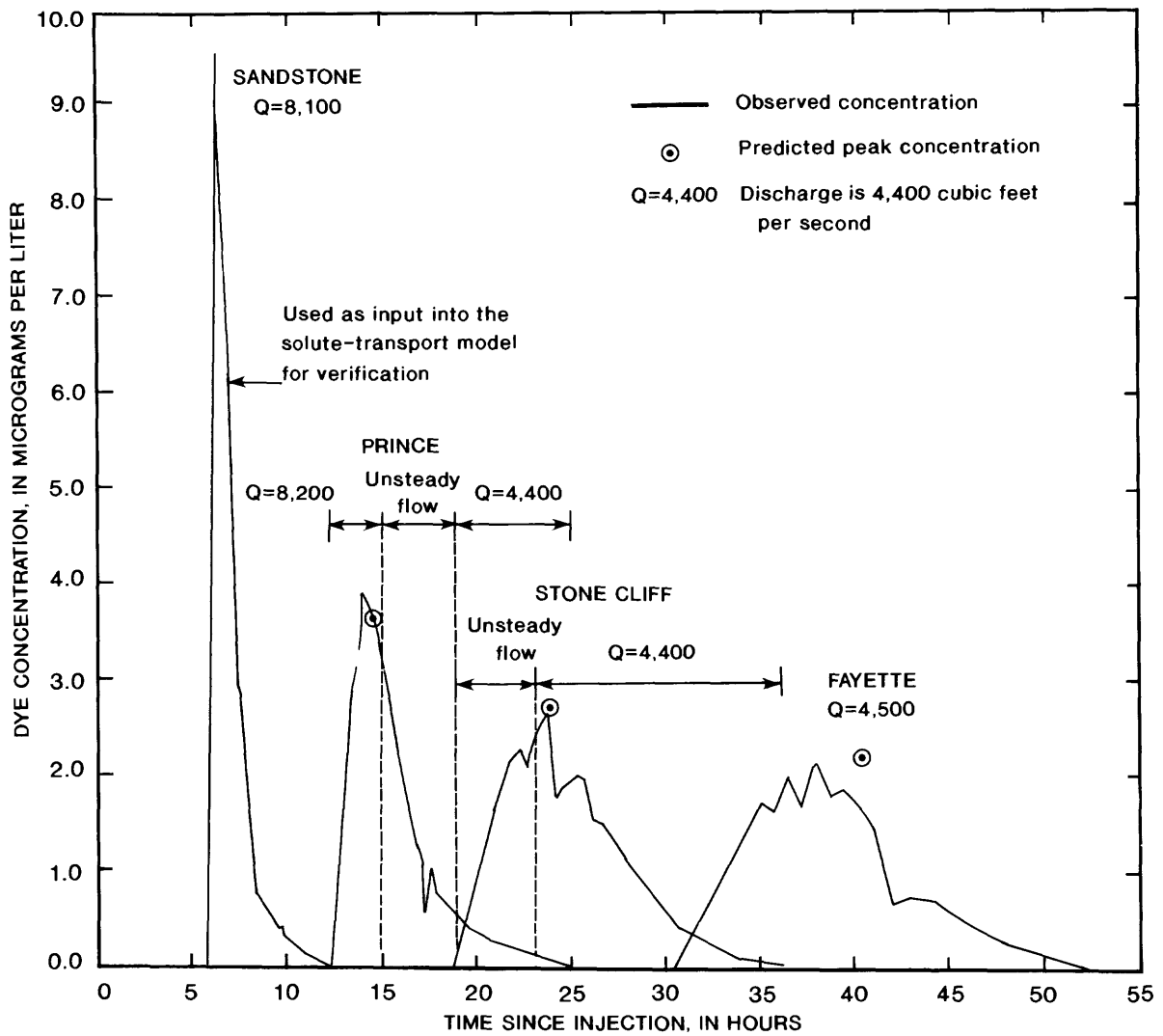

Figure 8.--Predicted and observed peak concentrations and traveltimes of peak concentrations for decreasing unsteady flow. (Modified from Wiley and Appel, 1989, p. 11.)

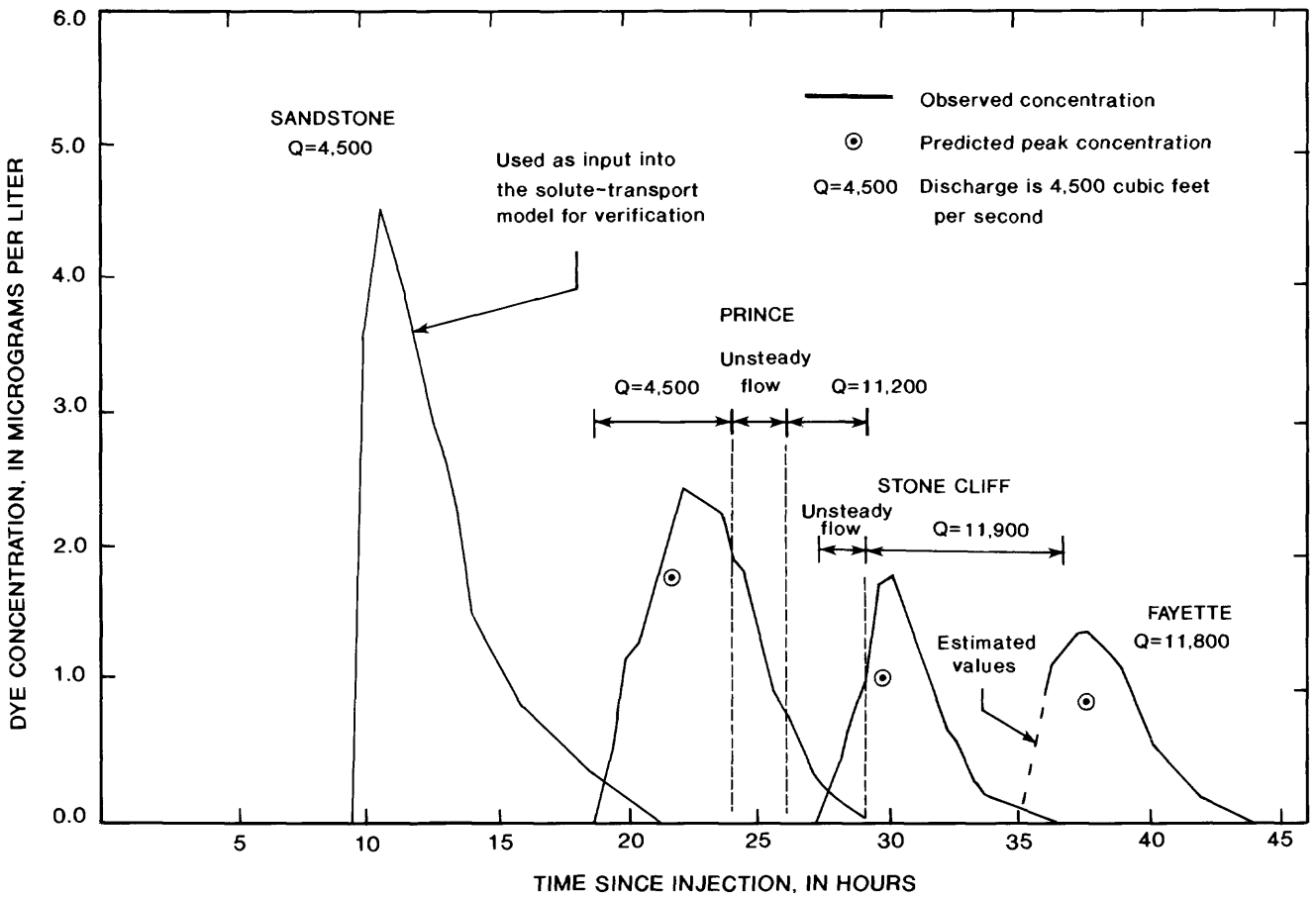

Figure 9.--Predicted and observed peak concentrations and traveltimes of peak concentrations for increasing unsteady flow. (Modified from Appel, 1987, p. 68.)

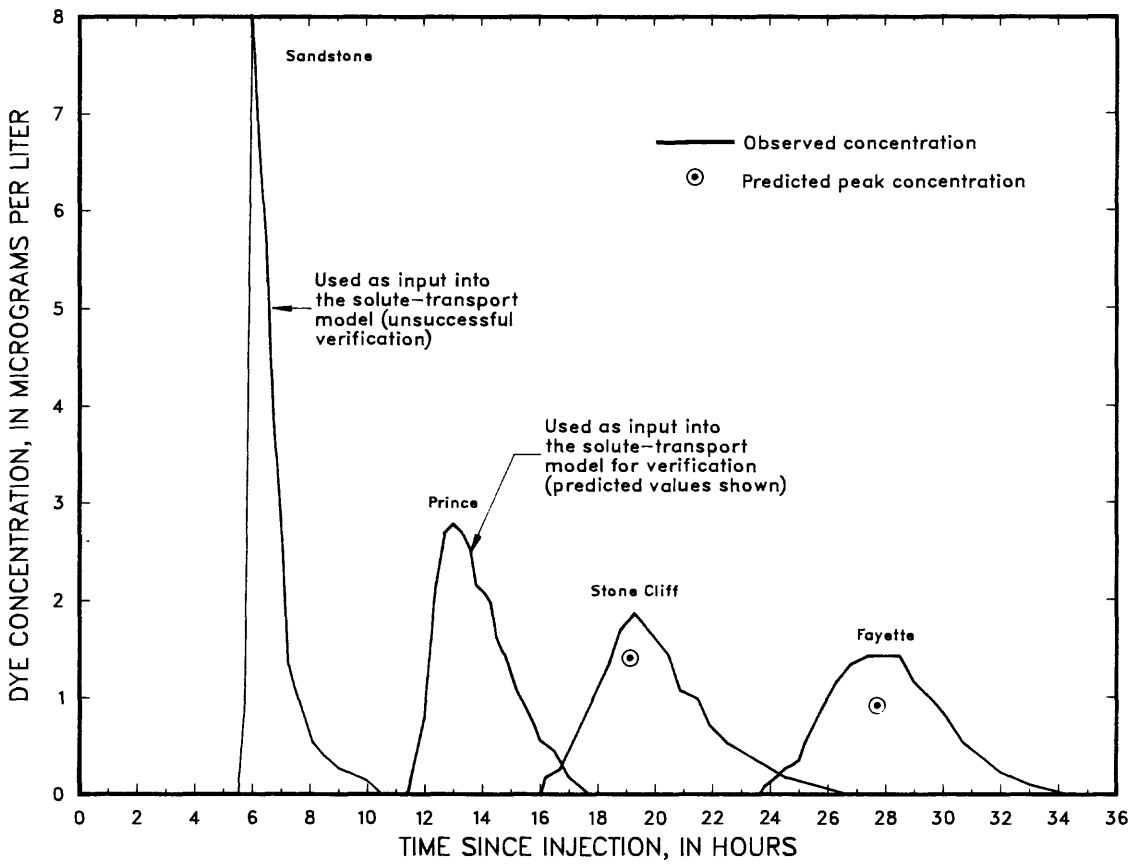

Figure 10.--Predicted and observed peak concentrations and traveltimes of peak concentrations for the May 1986 steady-flow study. (Modified from Appel and Moles, 1987, p. 4.)

The initial output from the high-discharge solute-transport model predicted a peak concentration at Prince of about one-half of what was observed. Reviewing the dye measurement records, the author discovered that mixing was incomplete when measurements were made at Sandstone. A composite sample from three observation points across the I-64 bridge at Sandstone had a peak concentration of 6.44 µg/L (a concentration of 8.0 µg/L is reported in fig. 10). Data also indicated that the dye cloud was traveling close to the left bank. An attempt was made to verify the model by use of the composite concentrations from records of the dye measurement, but the predicted concentrations were not significantly increased. The model could not be verified with dye data at Sandstone to predict peak concentrations and the traveltimes of peak concentrations at Prince, Stone Cliff, and Fayette.

Because the model could not be verified with data from Sandstone, verification was attempted by use of observed dye data from Prince. This required that the high-discharge solute-transport model be modified from three to two branches. Two branches are necessary because the solute-transport model requires the input-concentration curve to be at the most upstream grid. The output from the high-discharge unsteady-flow model also was modified to fit the two-branch network.

The initial run of the two-branch high-discharge solute-transport model predicted the traveltime of peak concentration at Fayette to be 2 hours later than what was observed. Reviewing the dye-measurement records, the author noted that considerable inflow was indicated by comparison of discharges between the Hinton and Thurmond streamflow-gaging stations. The average discharge of the dye measurement was 9,200 ft^3/s, but at the Thurmond gage, discharge was 10,800 ft^3/s while the dye cloud was in the lower areas of the study reach. The two-branch high-discharge solute-transport model was rerun with a steady discharge of 10,800 ft^3/s.

The predicted and observed concentrations are shown in figure 10. The predicted concentrations are less than the observed concentrations. These differences could be attributed to the fact that (1) the dye data at Prince indicate that the dye cloud was still concentrated near the left bank, and (2) the calibration of the high-discharge solute-transport model predicts concentrations approximately 10 percent lower than the observed concentrations at a discharge of 10,000 ft^3/s (table 20).

Sensitivity

The parameters A0 and DQQ were increased and decreased by 20 percent (tables 21-24) and time steps were increased and decreased by 50 percent (tables 25 and 26) to study sensitivity of the solute-transport model. Parameters W1 and W2 do not affect model results because they only affect decay computations that were not executed; hence, sensitivity to adjustments of W1 and W2 is not reported. (W1 and W2 were adjusted in several runs of the model to ensure that they made no difference in model output.)

As A0 increases, peak concentrations decrease and the traveltimes of peak concentrations increase (table 21). As A0 decreases, peak concentrations increase and the traveltimes of peak concentrations decrease (table 22). The magnitude of the differences is approximately the same for peak concentration and the traveltime of peak concentration when A0 is increased and decreased. The models are more sensitive to adjustments of A0 at low discharges than at high discharges. In addition, there is an accumulative effect in the downstream direction.

As DQQ increases, peak concentrations decrease, and as DQQ decreases, peak concentrations increase (tables 23 and 24). Adjusting DQQ does not significantly affect the traveltime of peak concentration as compared to the effect on peak concentration. On the basis of sensitivity-test results, there is a tendency for the traveltime of peak concentration to decrease when DQQ is increased and for the traveltime of peak concentration to increase when DQQ is decreased.

Increasing and decreasing time steps indicated more sensitivity at high discharges than at low discharges when predicting peak concentrations (tables 25 and 26). No trend was established for adjusting time step to predict the traveltimes of peak concentrations.

Peak concentration is least sensitive to adjustments of time step and about equally sensitive to adjustments of A0 and DQQ. The prediction of the traveltime of peak concentration is least sensitive to adjustments of DQQ, more sensitive to adjustments of time step, and most sensitive to adjustments of A0.

Table 21.--*Differences between predicted peak concentrations and those of the calibrated solute-transport models, and between predicted traveltimes of peak concentrations and those of the calibrated solute-transport models when average cross-sectional area of zero flow (A0) is increased by 20 percent*

[TT, the traveltime of peak concentration. PC, peak concentration. ft^3/s, cubic feet per second. All differences in peak concentration are in percent. All differences in traveltime are in 0.2 hour time step. Positive values indicate the model predicts a higher peak concentration or traveltime of peak concentration than the measured concentration or traveltime. Negative values indicate the model predicts a lower peak concentration or traveltime of peak concentration than the measured concentration or traveltime.]

Location	Difference in peak concentration and traveltime for a given solute-transport model and discharge							
	Low-discharge model				High-discharge model			
	3,000 ft^3/s		5,000 ft^3/s		10,000 ft^3/s		22,800 ft^3/s	
	TT	PC	TT	PC	TT	PC	TT	PC
Sandstone	+2	-2	+1	-1	+1	-2	0	0
Prince	+5	-6	+8	-6	0	-4	0	0
Stone Cliff	+7	-7	+8	-7	+4	-5	+1	-2
Fayette	+29	-7	+19	-7	+6	-5	+2	-3

Table 22.--*Differences between predicted peak concentrations and those of the calibrated solute-transport models, and between predicted traveltimes of peak concentrations and those of the calibrated solute-transport models when average cross-sectional area of zero flow (A0) is decreased by 20 percent*

[TT, the traveltime of peak concentration. PC, peak concentration. ft^3/s, cubic feet per second. All differences in peak concentration are in percent. All differences in traveltime are in 0.2 hour time step. Positive values indicate the model predicts a higher peak concentration or traveltime of peak concentration than the measured concentration or traveltime. Negative values indicate the model predicts a lower peak concentration or traveltime of peak concentration than the measured concentration or traveltime.]

Location	Difference in peak concentration and traveltime for a given solute-transport model and discharge							
	Low-discharge model				High-discharge model			
	3,000 ft^3/s		5,000 ft^3/s		10,000 ft^3/s		22,800 ft^3/s	
	TT	PC	TT	PC	TT	PC	TT	PC
Sandstone	-3	+3	-3	+2	0	+1	0	0
Prince	-13	+7	-5	+6	-3	+5	-2	+2
Stone Cliff	-22	+7	-10	+8	-2	+4	-4	+4
Fayette	-31	+9	-18	+8	-7	+4	-3	+4

Table 23.--*Differences between predicted peak concentrations and those of the calibrated solute-transport models, and between predicted traveltimes of peak concentrations and those of the calibrated solute-transport models when the dispersion factor (DQQ) is increased by 20 percent*

[TT, the traveltime of peak concentration. PC, peak concentration. ft^3/s, cubic feet per second. All differences in peak concentration are in percent. All differences in traveltime are in 0.2 hour time step. Negative values indicate the model predicts a lower peak concentration or traveltime of peak concentration than the measured concentration or traveltime.]

Location	Difference in peak concentration and traveltime for a given solute-transport model and discharge							
	Low-discharge model				High-discharge model			
	3,000 ft^3/s		5,000 ft^3/s		10,000 ft^3/s		22,800 ft^3/s	
	TT	PC	TT	PC	TT	PC	TT	PC
Sandstone	0	-3	-1	-5	0	-6	0	-6
Prince	0	-5	0	-6	0	-7	-1	-7
Stone Cliff	-6	-5	0	-7	0	-7	0	-8
Fayette	0	-6	0	-7	-1	-7	-1	-7

Table 24.--*Differences between predicted peak concentrations and those of the calibrated solute-transport models, and between predicted traveltimes of peak concentrations and those of the calibrated solute-transport models when the dispersion factor (DQQ) is decreased by 20 percent*

[TT, the traveltime of peak concentration. PC, peak concentration. ft^3/s, cubic feet per second. All differences in peak concentration are in percent. All differences in traveltime are in 0.2 hour time step. Positive values indicate the model predicts a higher peak concentration or traveltime of peak concentration than the measured concentration or traveltime.]

Location	Difference in peak concentration and traveltime for a given solute-transport model and discharge							
	Low-discharge model				High-discharge model			
	3,000 ft^3/s		5,000 ft^3/s		10,000 ft^3/s		22,800 ft^3/s	
	TT	PC	TT	PC	TT	PC	TT	PC
Sandstone	0	+4	0	+6	0	+11	+1	+8
Prince	0	+6	0	+8	0	+9	0	+10
Stone Cliff	0	+7	0	+9	+2	+10	0	+11
Fayette	+2	+7	+2	+9	+1	+10	0	+10

Table 25.--*Differences between predicted peak concentrations and those of the calibrated solute-transport models, and between predicted traveltimes of peak concentrations and those of the calibrated solute-transport models when time step is increased by 50 percent*

[TT, the traveltime of peak concentration. PC, peak concentration. ft^3/s, cubic feet per second. All differences in peak concentration are in percent. All differences in traveltime are in 0.2 hour time step. Positive values indicate the model predicts a higher peak concentration or traveltime of peak concentration than the measured concentration or traveltime. Negative values indicate the model predicts a lower peak concentration or traveltime of peak concentration than the measured concentration or traveltime.]

Location	Difference in peak concentration and traveltime for a given solute-transport model and discharge							
	Low-discharge model				High-discharge model			
	3,000 ft^3/s		5,000 ft^3/s		10,000 ft^3/s		22,800 ft^3/s	
	TT	PC	TT	PC	TT	PC	TT	PC
Sandstone	0	-6	-1	-10	-1	-10	-1	-11
Prince	-5	0	0	+3	0	+2	-2	-13
Stone Cliff	-3	+1	0	+6	0	-4	-1	-10
Fayette	+1	+1	+1	0	0	-7	0	-7

Table 26.--*Differences between predicted peak concentrations and those of the calibrated solute-transport models, and between predicted traveltimes of peak concentrations and those of the calibrated solute-transport models when time step is decreased by 50 percent*

[TT, the traveltime of peak concentration. PC, peak concentration. ft^3/s, cubic feet per second. All differences in peak concentration are in percent. All differences in traveltime are in 0.2 hour time step. Positive values indicate the model predicts a higher peak concentration or traveltime of peak concentration than the measured concentration or traveltime. Negative values indicate the model predicts a lower peak concentration or traveltime of peak concentration than the measured concentration or traveltime.]

Location	Difference in peak concentration and traveltime for a given solute-transport model and discharge							
	Low-discharge model				High-discharge model			
	3,000 ft^3/s		5,000 ft^3/s		10,000 ft^3/s		22,800 ft^3/s	
	TT	PC	TT	PC	TT	PC	TT	PC
Sandstone	-4	+2	-1	+3	-2	-6	+1	+10
Prince	+1	0	+1	0	+4	+2	-2	+4
Stone Cliff	+1	0	+1	0	+8	+4	-2	+7
Fayette	+1	+1	+2	0	+7	+3	-1	+9

COMPARISON OF RELATIONS DEVELOPED FROM MODELS

Output from the steady-flow model was evaluated and compared with calibration parameters A0, A1, and A2 from the unsteady-flow models. River volumes presented in table 3 were converted to average cross-sectional areas by dividing by the length of the applicable river reach (table 27). A log-log plot of average cross-sectional area minus average cross-sectional area of zero discharge as a function of discharge should be a straight line (figs. 11-14).

The plots (figs. 11-14) are nearly straight lines except for the areas minus cross-sectional areas of zero discharge calculated at 100 ft^3/s in the Hinton-to-Meadow Creek and Sewell-to-Fayette subreaches. For both of these subreaches, the area minus area of zero discharge is too low to develop a straight line.

Equation 3 from the user's manual for the unsteady-flow model (Jobson, 1989, p. 3) can be modified as follows:

$$A - A0 = A1 * QS^{A2},$$

where

A is the average cross-sectional area of flow, and

QS is the steady-flow discharge that corresponds to the average cross-sectional area (A).

This is a power function where a log-log plot of A1 QS^{A2} is a straight line.

Table 27.--*Average cross-sectional areas calculated by use of the steady-flow model*

[ft^3/s, cubic feet per second. Areas are in square feet.]

River reach	Cross-sectional area for a given discharge						
	0	100 ft^3/s	1,000 ft^3/s	5,000 ft^3/s	10,000 ft^3/s	28,000 ft^3/s	80,000 ft^3/s
Hinton to Meadow Creek	593	682	1,130	2,140	2,940	5,000	9,280
Meadow Creek to Sewell	1,010	1,110	1,500	2,360	3,060	4,970	8,980
Sewell to Fayette	1,140	1,290	1,650	2,490	3,140	4,760	8,110
Entire study reach	924	1,030	1,430	2,330	3,050	4,950	8,930

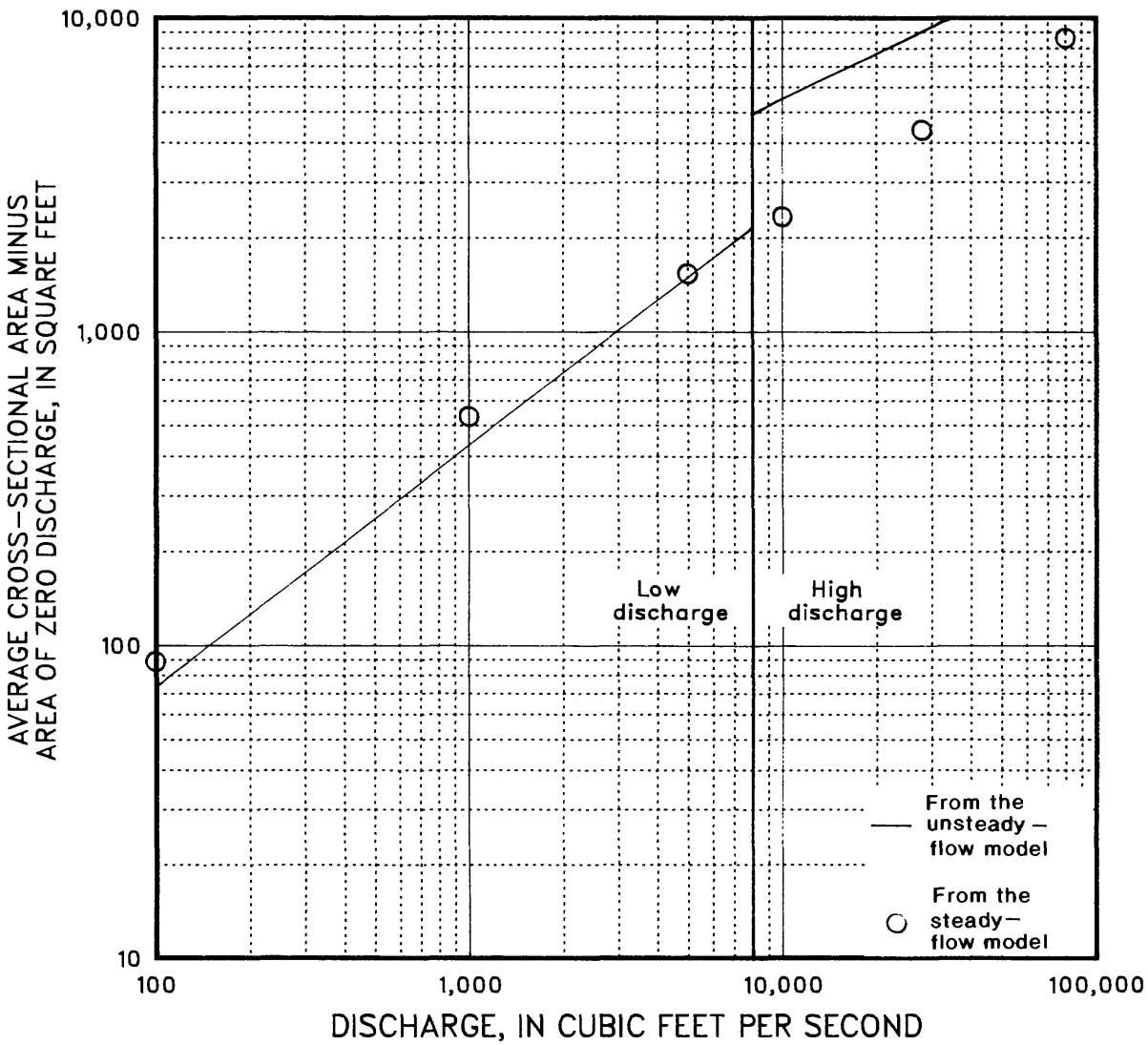

Figure 11.--Relations between discharge and average cross-sectional area of zero discharge for the Hinton-to-Meadow Creek subreach.

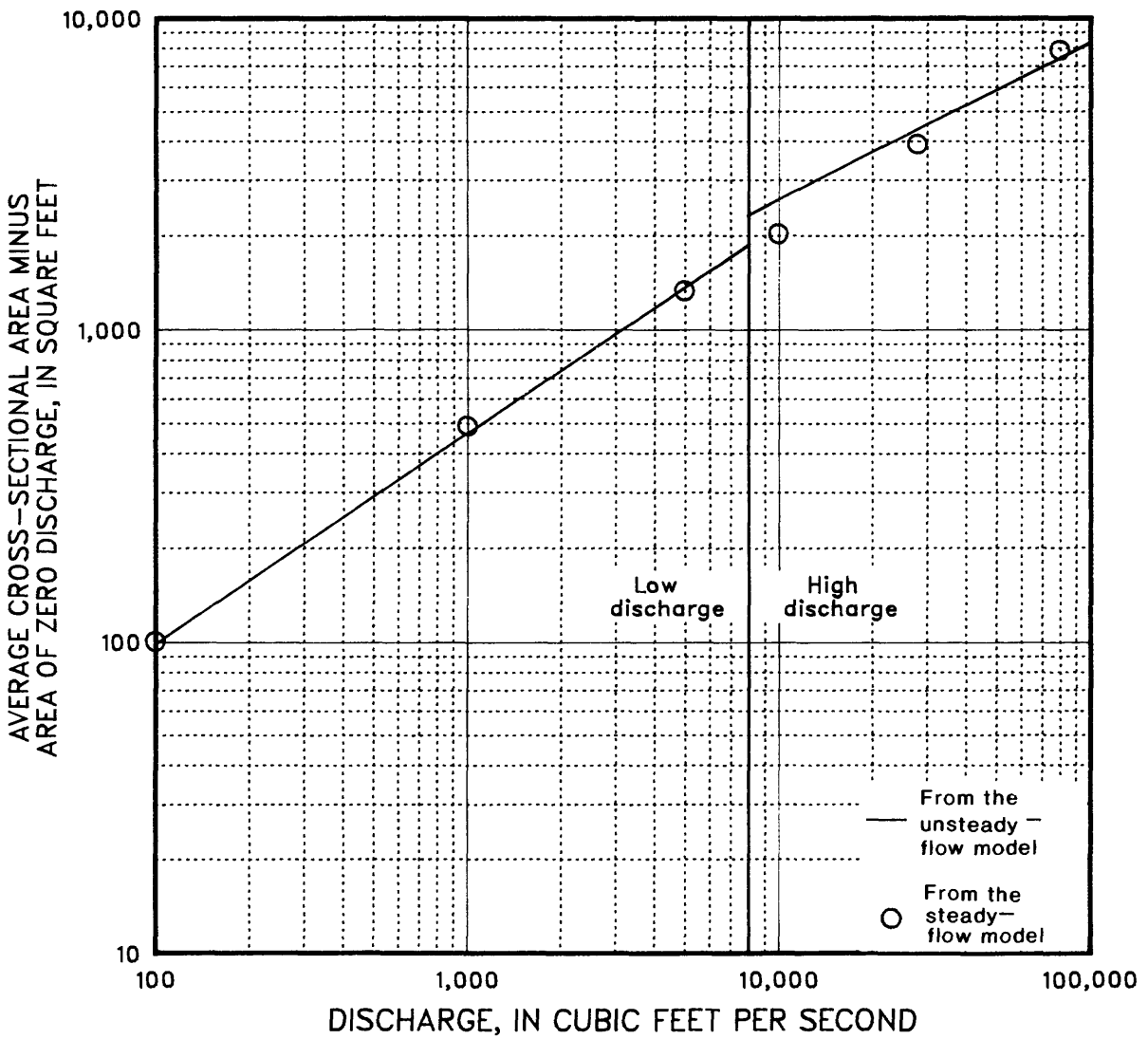

Figure 12.--Relations between discharge and average cross-sectional area of zero discharge for the Meadow Creek-to-Sewell subreach.

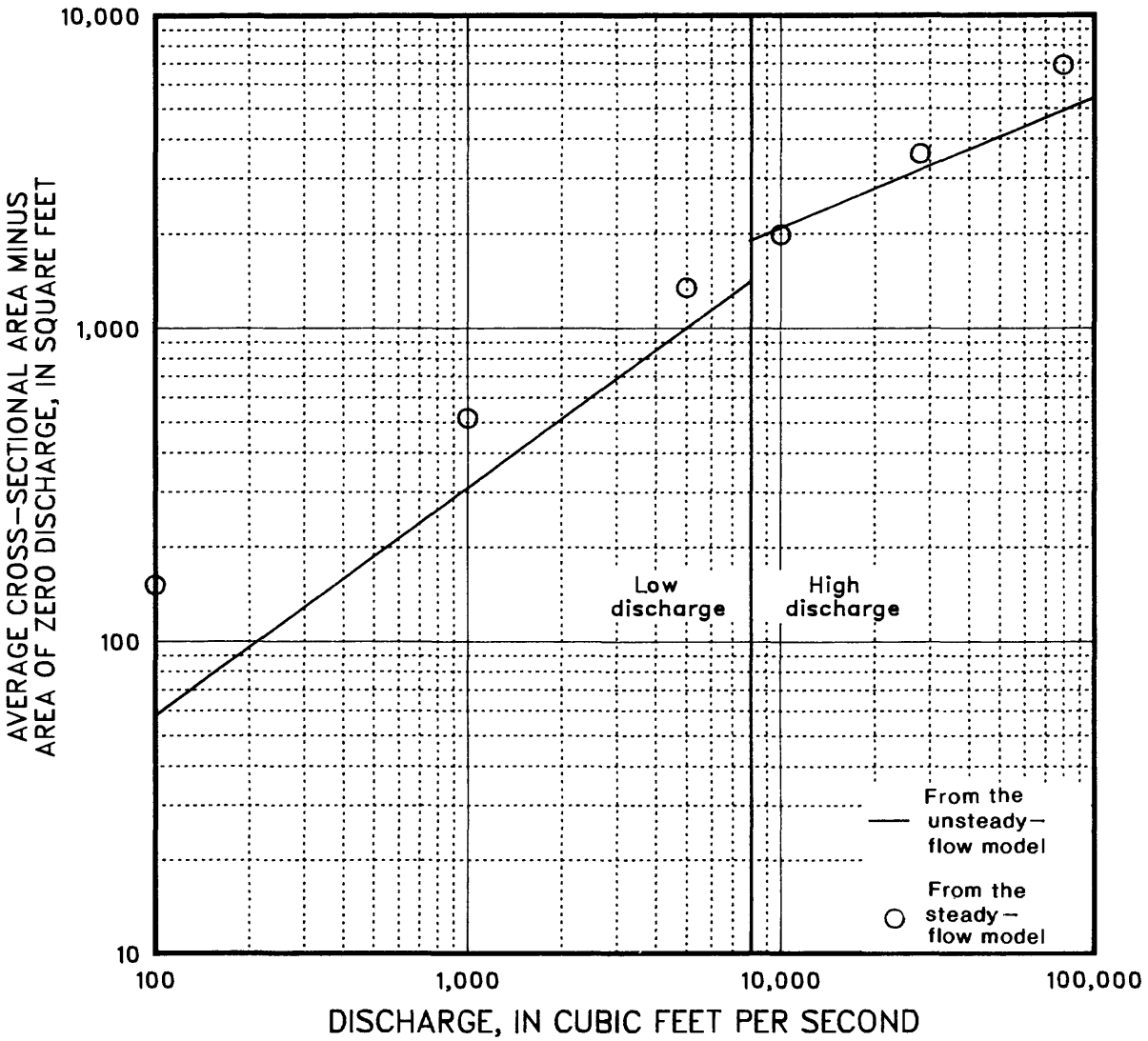

Figure 13.--Relations between discharge and average cross-sectional area of zero discharge for the Sewell-to-Fayette subreach.

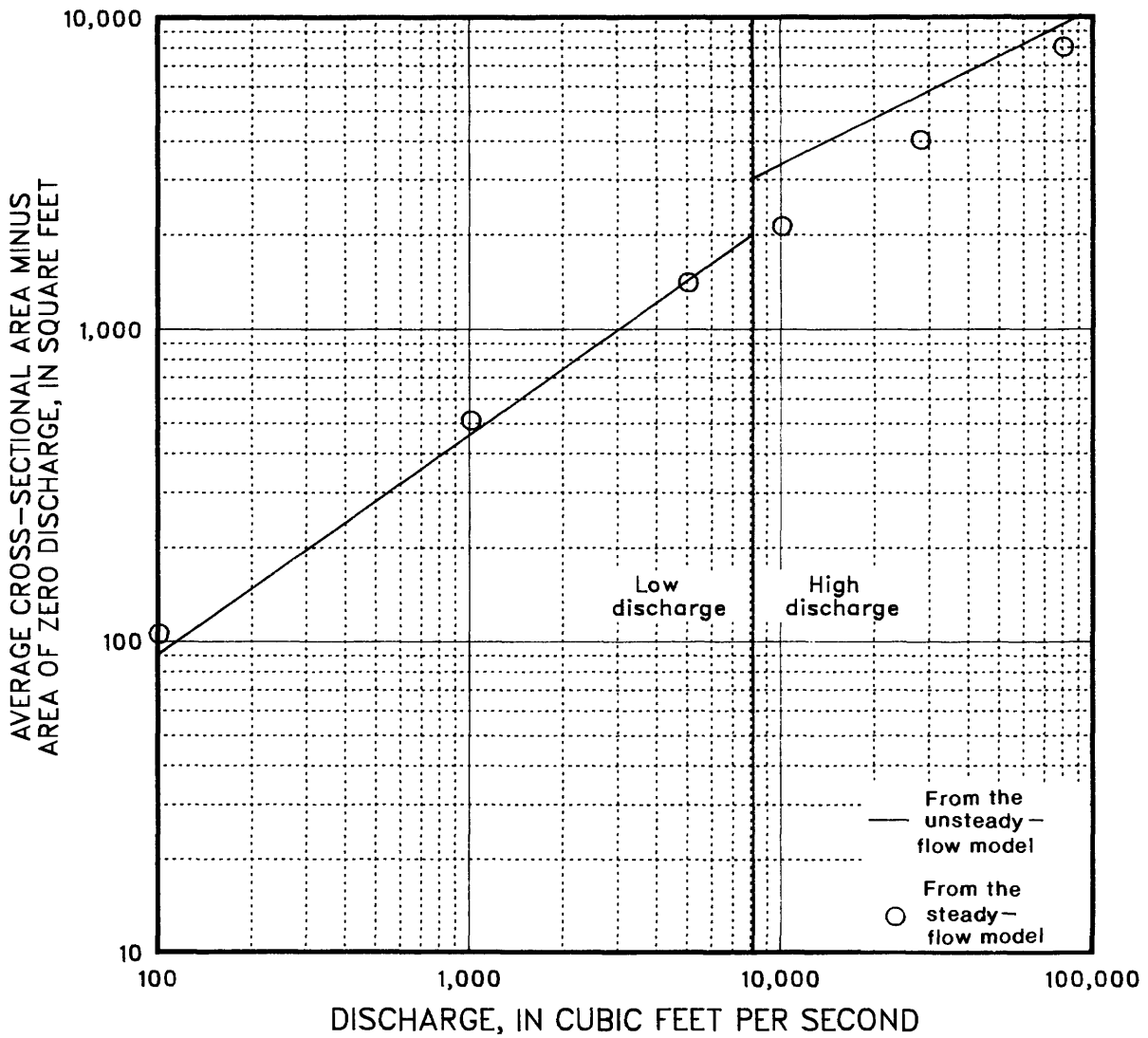

Figure 14.--Relations between discharge and average cross-sectional area of zero discharge for the entire study reach.

Table 28 shows A0, A1, and A2 for each subreach and for the entire study reach. These values are weighted averages based on the length of the applicable river reach of the calibration parameters A0, A1, and A2 for the unsteady-flow models (appendixes A and B). For each river reach, the low-discharge model values for A1 are less than those for the high-discharge model, and the low-discharge model values for A2 are greater than those for the high-discharge model. No explanation is apparent for this trend.

Relations from table 28 are shown on figures 11-14 to compare values computed from steady-flow model output to parameters used to calibrate the unsteady-flow model. Generally, for a given discharge, the average cross-sectional area minus area of zero discharge is greater for the high-discharge unsteady-flow model relation than for the relation calculated from the steady-flow model output. Similarly, for a given discharge, the average area minus area of zero discharge is less for the low-discharge unsteady-flow model relation than for the relation calculated from the steady-flow model output. The parameter A2 is the slope of the relation for the unsteady-flow models. The slopes of the high-discharge unsteady-flow model relations are less than the slopes of the relations determined from the steady-flow model output. The slopes of the low-discharge unsteady-flow model relations are greater than the slopes determined from the steady-flow model output. The best comparison of values of area minus area of zero discharge between relations calculated from the steady-flow model output and the unsteady-flow model relations is at 8,000 ft^3/s. The low-discharge unsteady-flow model was calibrated at 8,000 ft^3/s, and errors in the traveltime of waves were balanced between two discharges less than 8,000 ft^3/s.

During calibration of the high-discharge solute-transport model, A0 was given the value of zero, and the traveltime of peak concentration predicted by the solute-transport model at Sandstone was greater than the measured traveltime of peak concentration at Sandstone. From figure 11, for the high-discharge unsteady-flow model, the area minus area of zero discharge is greater than twice that calculated from steady-flow model output at 8,000 ft^3/s. If the area minus area of zero discharge for the high-discharge unsteady-flow model were less, then it would compare better to values calculated from the steady-flow model output, and the traveltime of peak concentration predicted by the solute-transport model at Sandstone would be reduced. This reduction in predicted traveltime of peak concentration might make calibration of the high-discharge solute-transport model between Hinton and Sandstone possible.

The reason why unsteady-flow model relations and the relations determined from steady-flow model output compare so poorly is not understood.

Table 28.--*Relations between discharge and average cross-sectional area minus area of zero discharge from the unsteady-flow model parameters*

[A is the average cross-sectional area, in square feet. QS is the steady-flow discharge that corresponds to the average cross-sectional area (A), in cubic feet per second.]

River reach	Relation for a given unsteady-flow model	
	Low-discharge model	High-discharge model
Hinton to Meadow Creek	$A - 440 = 2.065 * QS^{0.774}$	$A - 440 = 62.9 * QS^{0.486}$
Meadow Creek to Sewell	$A - 1{,}500 = 4.46 * QS^{0.637}$	$A - 800 = 25.05 * QS^{0.505}$
Sewell to Fayette	$A - 2{,}200 = 2.01 * QS^{0.730}$	$A - 2{,}750 = 22.00 * QS^{0.497}$
Entire study reach	$A - 1{,}340 = 3.51 * QS^{0.706}$	$A - 993 = 34.02 * QS^{0.499}$

SUMMARY

Three U.S. Geological Survey computer models, a steady-flow model, an unsteady-flow model, and a solute-transport model, were applied in the New River Gorge National River, West Virginia to compare area/discharge relations developed from parameters used in the unsteady-flow model to area/discharge relations developed from the steady-flow model output.

The study reach is 53 mi of the lower New River from Hinton to Fayette. The study reach narrows, steepens, and deepens in the downstream direction. Three subreaches--Hinton to Meadow Creek, Meadow Creek to Sewell, and Sewell to Fayette--can represent similar slopes, geometries, and roughnesses of the study reach.

The steady-flow model, WSPRO (Water Surface PROfile), was calibrated by use of relations developed from measurements between stages and discharges throughout the study reach. Manning's roughness coefficients and associated hydraulic depths were adjusted until simulated water-surface elevations matched the rated water-surface elevations for specific discharges. Cross sections for the model were estimated by means of aerial photography, topographic maps, rating curves, and water-surface and streambed profiles. The model was verified by comparing random predicted water-surface elevations at 2,000 ft^3/s to those of a surveyed profile. The model was more sensitive to changes in Manning's roughness coefficients than to changes in hydraulic depth. The area of zero discharge and a relation between area and discharge were calculated from steady-flow model output for comparison to parameters of the unsteady-flow models.

The unsteady-flow models, DAFLOW (Diffusion Analogy FLOW), were calibrated by use of relations developed from measurements between the traveltime of waves and discharge. Difficulty in calibration required development of separate models for discharges greater than or equal to 8,000 ft^3/s (high-discharge model) and less than or equal to 8,000 ft^3/s (low-discharge model). The models were verified by predicting discharges at the Thurmond streamflow-gaging station by means of inputing discharges from the Hinton station. The models were most sensitive to adjustments of the parameter A1.

The solute-transport models, BLTM (Branch Lagrangian Transport Model), were calibrated by use of the relations between the traveltime of peak concentration and discharge, and peak concentration and the traveltime of peak concentration. The models were verified by predicting peak concentrations and the traveltimes of peak concentrations for two unsteady-flow and one steady-flow dye measurements. The models were most sensitive to adjustments of A0 (average cross-sectional area at zero discharge) when predicting the traveltime of the peak concentration and were about as equally sensitive to adjustments of A0 and DQQ (dispersion factor) when predicting peak concentrations.

River volumes calculated from the steady-flow model output were converted to average cross-sectional areas and then compared to unsteady-flow parameters A0, A1, and A2 (hydraulic geometry exponent for area). A poor comparison resulted; no explanation could be determined for these anomalies.

REFERENCES CITED

Appel, D.H., 1983, Traveltimes of flood waves on the New River between Hinton and Hawks Nest, West Virginia: U.S. Geological Survey Water-Supply Paper 2225, 14 p.

____1987, Solute traveltime and dispersion in the New River, West Virginia, in New River Symposium, 1987, Proceedings: National Park Service, p. 59-70.

Appel, D.H., and **Moles, S.B.**, 1987, Traveltime and dispersion in the New River, Hinton to Gauley Bridge, West Virginia: U.S. Geological Survey Water-Resources Investigations Report 87-4012, 21 p.

Barnes, H.H. Jr., 1967, Roughness characteristics of natural channels: U.S. Geological Survey Water-Supply Paper 1849, 213 p.

Jobson, H.E., and **Schoellhamer, D.H.**, 1987, User's manual for a branched Lagrangian transport model: U.S. Geological Survey Water-Resources Investigations Report 87-4163, 73 p.

Jobson, H.E., 1989, Users manual for an open-channel streamflow model based on the diffusion analogy: U.S. Geological Survey Water-Resources Investigations Report 89-4133, 73 p.

Mathes, M.V., **Kirby, J.R.**, **Payne, Jr.**, and **Shultz, R.A.**, 1982, Drainage areas of the Kanawha River basin, West Virginia: U.S. Geological Survey Open-File Report 82-351, 222 p.

Shearman, J.O., **Kirby, W.H.**, **Schneider, V.R.**, and **Flippo, H.N.**, 1986, Bridge waterways analysis model--research report: U.S. Department of Transportation, Federal Highway Administration Report FHWA/RD-86/108, 112 p.

Wiley, J.B., and **Appel, D.H.**, 1989, Hydraulic characteristics of the New River in the New River Gorge National River, West Virginia: U.S. Geological Survey Open-File Report 89-243, 34 p.

Wiley, J.B., 1989, River depths and other characteristics of the New River downstream from Hinton, West Virginia, in New River Symposium, 1989, Proceedings: National Park Service, p. 129-139.

APPENDIXES

APPENDIX A

Part of the Input File Containing Flow Parameters
for the Low-Discharge Unsteady-Flow Model

```
New River / low-flow DAFLOW FLOW.IN
No. of Branches                1 *
Internal Junctions             0 *
Time Steps Modeled           180 *
Model Starts                   0 time steps after midnight.
Output Given Every             1 Time Steps in FLOW.OUT.
0=Metric,1=English             1 *
Time Step Size             0.100 Hours.
Peak Discharge             90000. *
Branch  1 has 11 xsects & routes 1.00 of flow at JNCT  1 To JNCT  2
Grd R Mile   IOUT  Disch        A1         A2         AO         DF         W1     W2
  1 0.0000      1   2200.      2.44      0.760       440.      1568.      118.0 0.260
  2  9.470      1   2200.      1.08      0.810       440.      1568.      118.0 0.260
  3  10.43      0   2200.      1.08      0.810       440.      1568.      118.0 0.260
  4  13.07      1   2200.     6.431      0.630       440.      2423.       76.2 0.260
  5  23.86      1   2200.     3.448      0.690       440.      2423.       76.2 0.260
  6  36.14      0   2200.     3.448      0.690       440.      2423.       76.2 0.260
  7  37.58      1   2200.     3.448      0.690       440.      2423.       76.2 0.260
  8  44.87      0   2200.     2.010      0.730      2150.      1428.       48.5 0.260
  9  46.44      0   2200.     2.010      0.730      2150.      1428.       48.5 0.260
 10  51.36      1   2200.     2.010      0.730      2150.      1428.       48.5 0.260
 11  52.50      0
for Time     1 NBC=  1 *
 Branch      1 Grid  1 Q=      2400.0     *
for Time     2 NBC=  0 *
for Time     3 NBC=  0 *
for Time     4 NBC=  0 *
for Time     5 NBC=  0 *
.
.
.
.
.
.
for Time   175 NBC=  0 *
for Time   176 NBC=  0 *
for Time   177 NBC=  0 *
for Time   178 NBC=  0 *
for Time   179 NBC=  0 *
for Time   180 NBC=  0 *
```

APPENDIX B

Part of the Input File Containing Flow Parameters
for the High-Discharge Unsteady-Flow Model

```
New River / high-flow DAFLOW FLOW.IN
No. of Branches                1 *
Internal Junctions             0 *
Time Steps Modeled           180 *
Model Starts                   0 time steps after midnight.
Output Given Every             1 Time Steps in FLOW.OUT.
0=Metric,1=English             1 *
Time Step Size             0.100 Hours.
Peak Discharge             90000. *
Branch  1 has 11 xsects & routes 1.00 of flow at JNCT  1 To JNCT  2
Grd R Mile   IOUT  Disch        A1        A2        AO        DF        W1    W2
  1 0.0000      1  22800.     35.74     0.530      440.      3552.     118.0 0.260
  2  9.470      1  22800.     134.2     0.370      440.      3552.     118.0 0.260
  3  10.43      0  22800.     134.2     0.370      440.      3552.     118.0 0.260
  4  13.07      1  22800.     22.00     0.514      440.      5490.      76.2 0.260
  5  23.86      1  22800.     26.63     0.500      440.      5490.      76.2 0.260
  6  36.14      0  22800.     26.63     0.500      440.      5490.      76.2 0.260
  7  37.58      1  22800.     26.63     0.500      440.      5490.      76.2 0.260
  8  44.87      0  22800.     22.00     0.497     2150.      3235.      48.5 0.260
  9  46.44      0  22800.     22.00     0.497     2150.      3235.      48.5 0.260
 10  51.36      1  22800.     22.00     0.497     2150.      3235.      48.5 0.260
 11  52.50      0
for Time     1 NBC=  1 *
 Branch      1 Grid  1 Q=     25000.0    *
for Time     2 NBC=  0 *
for Time     3 NBC=  0 *
for Time     4 NBC=  0 *
for Time     5 NBC=  0 *
.
.
.
.
.
for Time   175 NBC=  0 *
for Time   176 NBC=  0 *
for Time   177 NBC=  0 *
for Time   178 NBC=  0 *
for Time   179 NBC=  0 *
for Time   180 NBC=  0 *
```

APPENDIX C

Part of the Input File Containing Transport Parameters for the High-Discharge Solute-Transport Model

```
New River / high-flow BLTM.IN
HEADER 1          3       2     350       1       0       1       1       0       1
HEADER 2       0.20    0.00
LABEL             1    DYE        1
BRANCH    1       4    0.75       3       1      50
 GRID     1   0.000       0    0.00
 GRID     2   9.470       0    0.00
 GRID     3  10.430       1    0.00
 GRID     4  13.070       0
BRANCH    2       5    1.30       1       2      40
 GRID     1  13.070       0    0.00
 GRID     2  23.860       1    0.00
 GRID     3  36.140       1    0.00
 GRID     4  37.580       0    0.00
 GRID     5  44.870       0
BRANCH    3       4    1.50       2       4      40
 GRID     1  44.870       0    0.00
 GRID     2  46.440       0    0.00
 GRID     3  51.360       1    0.00
 GRID     4  52.500       1
TIME      1       1
 B  1 G  1    0.00
.
.
.
TIME     29       1
 B  1 G  1    0.00
TIME     30       1
 B  1 G  1    6.20
TIME     31       1
 B  1 G  1    9.40
TIME     32       1
 B  1 G  1    8.33
TIME     33       1
 B  1 G  1    7.27
.
.
.
TIME     43       1
 B  1 G  1    0.34
TIME     44       1
 B  1 G  1    0.00
.
.
.
TIME    350       1
 B  1 G  1    0.00
```

APPENDIX D

Part of the Input File Containing Flow Parameters
for the High-Discharge Solute-Transport Model

```
New River / high-flow BLTM FLOW.IN
No. of Branches                1 *
Internal Junctions             0 *
Time Steps Modeled           350 *
Model Starts                   0 time steps after midnight.
Output Given Every             1 Time Steps in FLOW.OUT.
0=Metric,1=English             1 *
Time Step Size             0.200 Hours.
Peak Discharge             90000. *
Branch  1 has 11 xsects & routes 1.00 of flow at JNCT  1 To JNCT  2
Grd R Mile   IOUT  Disch        A1        A2        AO        DF        W1    W2
  1 0.0000      1  22800.     35.74     0.530      440.      3552.     118.0 0.260
  2  9.470      1  22800.     134.2     0.370      440.      3552.     118.0 0.260
  3  10.43      0  22800.     134.2     0.370      440.      3552.     118.0 0.260
  4  13.07      1  22800.     22.00     0.514      800.      5490.      76.2 0.260
  5  23.86      1  22800.     26.63     0.500      800.      5490.      76.2 0.260
  6  36.14      0  22800.     26.63     0.500      800.      5490.      76.2 0.260
  7  37.58      1  22800.     26.63     0.500      800.      5490.      76.2 0.260
  8  44.87      0  22800.     22.00     0.497     2750.      3235.      48.5 0.260
  9  46.44      0  22800.     22.00     0.497     2750.      3235.      48.5 0.260
 10  51.36      1  22800.     22.00     0.497     2750.      3235.      48.5 0.260
 11  52.50      0
for Time     1 NBC=  1 *
 Branch      1 Grid  1 Q=   22800.0     *
for Time     2 NBC=  0 *
for Time     3 NBC=  0 *
for Time     4 NBC=  0 *
for Time     5 NBC=  0 *
.
.
.
.
.
for Time   345 NBC=  0 *
for Time   346 NBC=  0 *
for Time   347 NBC=  0 *
for Time   348 NBC=  0 *
for Time   349 NBC=  0 *
for Time   350 NBC=  0 *
```

APPENDIX E

Part of the Input File Containing Transport Parameters for the Low-Discharge Solute-Transport Model

```
New River / low-flow BLTM BLTM.IN
HEADER 1        3      2    350      1      0      1      1      0      1
HEADER 2     0.20   0.00
LABEL           1   DYE       1
BRANCH   1      4   1.30      3      1     50
 GRID    1  0.000      0   0.00
 GRID    2  9.470      0   0.00
 GRID    3 10.430      1   0.00
 GRID    4 13.070      0
BRANCH   2      5   0.55      1      2     40
 GRID    1 13.070      0   0.00
 GRID    2 23.860      1   0.00
 GRID    3 36.140      1   0.00
 GRID    4 37.580      0   0.00
 GRID    5 44.870      0
BRANCH   3      4   1.50      2      4     40
 GRID    1 44.870      0   0.00
 GRID    2 46.440      0   0.00
 GRID    3 51.360      1   0.00
 GRID    4 52.500      1
TIME     1      1
 B  1 G  1   0.00
.
.
.
TIME    27      1
 B  1 G  1   0.00
TIME    28      1
 B  1 G  1   0.60
TIME    29      1
 B  1 G  1   1.30
TIME    30      1
 B  1 G  1   5.20
TIME    31      1
 B  1 G  1   7.80
TIME    32      1
 B  1 G  1   7.51
.
.
.
TIME    70      1
 B  1 G  1   0.00
.
.
.
TIME   350      1
 B  1 G  1   0.00
```

APPENDIX F

Part of the Input File Containing Flow Parameters
for the Low-Discharge Solute-Transport Model

```
New River / low-flow BLTM FLOW.IN
No. of Branches                1 *
Internal Junctions             0 *
Time Steps Modeled           350 *
Model Starts                   0 time steps after midnight.
Output Given Every             1 Time Steps in FLOW.OUT.
0=Metric,1=English             1 *
Time Step Size             0.200 Hours.
Peak Discharge           90000. *
Branch  1 has 11 xsects & routes 1.00 of flow at JNCT  1 To JNCT  2
Grd R Mile   IOUT  Disch        A1        A2        AO        DF        W1    W2
  1 0.0000      1   5000.      2.44     0.760      440.      1568.      118.0 0.260
  2  9.470      1   5000.      1.08     0.810      440.      1568.      118.0 0.260
  3  10.43      0   5000.      1.08     0.810      440.      1568.      118.0 0.260
  4  13.07      1   5000.     6.431     0.630     1500.      2423.       76.2 0.260
  5  23.86      1   5000.     3.448     0.690     1500.      2423.       76.2 0.260
  6  36.14      0   5000.     3.448     0.690     1500.      2423.       76.2 0.260
  7  37.58      1   5000.     3.448     0.690     1500.      2423.       76.2 0.260
  8  44.87      0   5000.     2.010     0.730     2200.      1428.       48.5 0.260
  9  46.44      0   5000.     2.010     0.730     2200.      1428.       48.5 0.260
 10  51.36      1   5000.     2.010     0.730     2200.      1428.       48.5 0.260
 11  52.50      0
for Time     1 NBC=  1 *
 Branch      1 Grid  1 Q=     5000.0    *
for Time     2 NBC=  0 *
for Time     3 NBC=  0 *
for Time     4 NBC=  0 *
for Time     5 NBC=  0 *
.
.
.
.
.
for Time   345 NBC=  0 *
for Time   346 NBC=  0 *
for Time   347 NBC=  0 *
for Time   348 NBC=  0 *
for Time   349 NBC=  0 *
for Time   350 NBC=  0 *
```